

Multisymplectic variational integrators for barotropic and incompressible fluid models with constraints

François Demoures¹ and François Gay-Balmaz²

February 23, 2021

Abstract

We present a structure preserving discretization of the fundamental spacetime geometric structures of fluid mechanics in the Lagrangian description in 2D and 3D. Based on this, multisymplectic variational integrators are developed for barotropic and incompressible fluid models, which satisfy a discrete version of Noether theorem. We show how the geometric integrator can handle regular fluid motion in vacuum with free boundaries and constraints such as the impact against an obstacle of a fluid flowing on a surface. Our approach is applicable to a wide range of models including the Boussinesq and shallow water models, by appropriate choice of the Lagrangian.

1 Introduction

This paper presents a multisymplectic variational integrator for barotropic fluids and incompressible fluids with free boundaries in the Lagrangian description. The integrator is derived from a spacetime discretization of the Hamilton principle of fluid dynamics and is based on a discrete version of the multisymplectic geometric formulation of continuum mechanics. As a consequence of its variational nature, the resulting scheme preserves exactly the momenta associated to symmetries, it is symplectic in time, and energy is well conserved. In addition to its conservative properties, the variational scheme can be naturally extended to handle constraints, such as the impact against an obstacle of fluid flowing on a surface, by augmenting the discrete Lagrangian with penalty terms.

Multisymplectic geometry is the natural geometric setting for classical field theories and is the appropriate spacetime extension of the symplectic formulation of classical mechanics. Important properties of Lagrangian and Hamiltonian systems in classical mechanics, such as the symplecticity of the flow and the preservation of the momentum

¹EPFL, Doc & Postdoc Alumni. Av Druey 1, Lausanne 1018, Switzerland
`francois.demoures@alumni.epfl.ch`

²CNRS & École Normale Supérieure, Laboratoire de Météorologie Dynamique, Paris, France.
`francois.gay-balmaz@lmd.ens.fr`

maps associated to symmetries, have corresponding statements for field theories that are intrinsically formulated via multisymplectic geometry. These are the *multisymplectic form formula* and the *covariant Noether theorem* for the solution of Euler-Lagrange field equations. Of particular importance in these formulations are the *Cartan forms* associated to the Lagrangian density of the theory.

Multisymplectic variational integrators were developed in [24] via a spacetime discretization of the Hamilton principle of field theories, which results in numerical schemes that satisfy a discrete version of the multisymplectic form formula and a discrete covariant Noether theorem. The discrete framework also allows the definitions of the concepts of *discrete Cartan forms* and *discrete covariant momentum maps*. Other approaches to multisymplectic integrators have been also developed, in, for example, [3]. We refer to [21, 8, 7, 9, 6] for the development of multisymplectic variational integrators for several mechanical systems of interest in engineering. Examples include the simulation of the dynamics of rotor blades via asynchronous variational integrators where it is necessary to compute accurate solutions for long periods of time, the dynamics of geometrically exact (Cosserat) beams, or the simulation of elastodynamic frictionless impact problems.

In this paper, we develop this method towards its application to compressible and incompressible fluid dynamics by using, at the continuous level, the multisymplectic variational formulation of continuum mechanics as described in [25, 15]. The main ingredients in our discrete approach are the concepts of discrete deformation gradient and discrete Jacobian, defined both in the 2D and 3D cases. They enter in a fundamental way in the definition of the spacetime discretized Lagrangian and they allow to exactly impose discrete incompressibility via an augmented Lagrangian approach. Besides its conservative properties, thanks to its variational nature, our scheme can be naturally extended to include constraints. This is illustrated with fluid flowing or impacting on a surface.

The variational discretization in this paper is carried out in the Lagrangian frame and for fluid dynamics interpreted as a special class of field theory on spacetime. Geometric variational discretizations for fluids have also been developed in the Eulerian description and for fluid dynamics interpreted as an infinite dimensional dynamical system on diffeomorphism groups, as opposed to the spacetime covariant description carried out here. This variational approach is based on a discretization of groups of diffeomorphisms, see [29, 30, 1, 16] for both incompressible and compressible models.

This paper is a first step towards the development of dynamic mesh update from a structure preserving point of view, inspired by arbitrary Lagrangian-Eulerian methods. Several approaches have been proposed in the literature, such as [20, 11, 12, 35, 27, 13].

The organization of the paper is as follows. Section §2 first briefly reviews the variational formulation of barotropic and incompressible fluid models in the Lagrangian description in a classical way. We mention in particular the case of isentropic perfect gas, the shallow water and Boussinesq equations, and the ideal fluid. This variational setting is then recasted in the multisymplectic variational formalism, which is fundamental for the discretization carried out later. The multisymplectic form formula and

the covariant Noether theorems are recalled. The two dimensional discrete fluid models are formulated in Section §3. In §3.1, the discrete configuration bundle and jet bundle are recalled, and the discrete deformation gradient, the discrete Jacobian as well as the discrete Lagrangian for barotropic models are defined. The discrete Euler-Lagrange equations are obtained from the discrete version of the Hamilton principle. The algorithmically conserved quantities (discrete multisymplectic form formula and Noether theorem) are written. In §3.2 discrete incompressibility is treated via a Lagrange multiplier constraint and via a penalty term. Numerical results are presented in §3.3 to demonstrate the basic properties of the method and to validate it, for both compressible and incompressible fluids, with free boundary or flowing on a surface and impacting against an obstacle. Section §4 develops the three dimensional discrete multisymplectic formulation for barotropic and incompressible ideal fluids with the same class of examples than in the two dimensional situation. The paper concludes with the Appendix A where several expressions needed to implement the integrators are given.

2 Barotropic and incompressible fluids

In this section we briefly review the variational formulation of barotropic and incompressible fluid models in the Lagrangian (or material) description in Cartesian coordinates. This formulation is then recasted in a multisymplectic variational setting, which allows to formulate intrinsically the Hamilton principle, the multisymplectic property of the solutions, and the covariant Noether theorem with the help of Cartan forms. This gives the geometric framework to be discretized in a structure preserving way later.

Assume that the reference configuration of the fluid is a compact domain $\mathcal{B} \subset \mathbb{R}^n$ with piecewise smooth boundary, and the fluid moves in the ambient space $\mathcal{M} = \mathbb{R}^n$. We denote by $\varphi : \mathbb{R} \times \mathcal{B} \rightarrow \mathcal{M}$ the fluid configuration map, which indicates the location $m = \varphi(t, X)$ at time t of the fluid particle with label $X \in \mathcal{B}$. The deformation gradient is denoted $\mathbf{F}(t, X)$, given in coordinates by $\mathbf{F}^a_i = \varphi^a_{,i}$, with $X^i, i = 1, \dots, n$ the Cartesian coordinates on \mathcal{B} and $m^a, a = 1, \dots, n$ the Cartesian coordinates on \mathcal{M} . We assume that the fluid configuration is regular enough so that all the computations below are valid.

2.1 Barotropic fluids

2.1.1 Definition

A fluid is *barotropic* if it is compressible and the surfaces of constant pressure p and constant density ρ coincide, i.e., we have a relation

$$p = p(\rho). \tag{1}$$

The internal energy W of barotropic fluids in the material description depends on the deformation gradient \mathbf{F} only through the Jacobian J of φ , given in Cartesian coordinates by

$$J(t, m) = \det(\mathbf{F}(t, X)),$$

hence in the material description we have $W = W(\rho_0, J)$, with $\rho_0(X)$ the mass density of the fluid in the reference configuration. The pressure in the material description is

$$P_W(\rho_0, J) = -\rho_0 \frac{\partial W}{\partial J}(\rho_0, J). \quad (2)$$

The *continuity equation for mass* can be written as

$$\rho_0(X) = \rho(t, \varphi(t, X))J(t, X), \quad (3)$$

with $\rho(t, m)$ the Eulerian mass density. The internal energy $w(\rho)$ in the Eulerian description satisfies the relation

$$W(\rho_0, J) = w\left(\frac{\rho_0}{J}\right)$$

and one notes that $P_W = p_w \circ \varphi$, with $p_w = \rho^2 \frac{\partial w}{\partial \rho}$ the Eulerian pressure p in (1).

2.1.2 Hamilton's principle for barotropic fluids

The Lagrangian of the barotropic fluid evaluated on a fluid configuration map $\varphi(t, X)$ has the standard form

$$L(\varphi, \dot{\varphi}, \nabla \varphi) = \frac{1}{2} \rho_0 |\dot{\varphi}|^2 - \rho_0 W(\rho_0, J) - \rho_0 \Pi(\varphi), \quad (4)$$

with Π a potential energy, such as the gravitational potential $\Pi(\varphi) = \mathbf{g} \cdot \varphi$.

Hamilton's principle

$$\delta \int_0^T \int_{\mathcal{B}} L(\varphi, \dot{\varphi}, \nabla \varphi) dt dX = 0$$

for variations of φ vanishing at $t = 0, T$ yields the Euler-Lagrange equations

$$\frac{\partial}{\partial t} \frac{\partial L}{\partial \dot{\varphi}} + \frac{\partial}{\partial x^i} \frac{\partial L}{\partial \varphi_{,i}} = \frac{\partial L}{\partial \varphi},$$

together with the natural boundary conditions

$$\frac{\partial L}{\partial \varphi_{,i}^a} n_i \delta \varphi^a = 0 \quad \text{on} \quad \partial \mathcal{B},$$

for allowed variations $\delta \varphi$. Here n denotes the outward pointing unit normal vector field to $\partial \mathcal{B}$.

From the Lagrangian of the barotropic fluid (4) and the material pressure P_W defined in (2) we get the barotropic fluid equations in the Lagrangian description as

$$\rho_0 \ddot{\varphi} + \frac{\partial}{\partial x^i} (P_W J \mathbf{F}^{-1})^i = -\rho_0 \frac{\partial \Pi}{\partial \varphi} \quad (5)$$

together with the natural boundary conditions

$$P_W J n_i (\mathbf{F}^{-1})_a^i \delta \varphi^a = 0 \quad \text{on} \quad \partial \mathcal{B}, \quad (6)$$

for all allowed variations $\delta \varphi$. For instance for a free boundary problem, the variations $\delta \varphi$ are arbitrary on $\partial \mathcal{B}$, hence the boundary condition (6) yields the zero pressure condition

$$P_W|_{\partial \mathcal{B}} = 0. \quad (7)$$

Boundary conditions with surface tension can be deduced from the Hamilton principle by adding an area term in the Lagrangian, see [17].

Using the relations $\dot{\varphi} = u \circ \varphi$, $P_W = p_w \circ \varphi$, and $\rho_0 = (\rho \circ \varphi)J$, between Lagrangian and Eulerian quantities, one deduces from (5) the familiar Eulerian form of barotropic fluids as

$$\rho(\partial_t u + u \cdot \nabla u) = -\nabla p_w - \rho \nabla \Pi, \quad \partial_t \rho + \text{div}(\rho u) = 0.$$

2.1.3 Example: isentropic perfect gas and rotating shallow water

Let us consider the following general barotropic expression for the internal energy and pressure

$$w(\rho) = \frac{A}{\gamma-1} \rho^{\gamma-1} + B \rho^{-1}, \quad p_w(\rho) = A \rho^\gamma - B, \quad (8)$$

for constants A , B , and adiabatic coefficient γ , see [5]. The material internal energy to be used in the Lagrangian (4) is

$$W(\rho_0, J) = \frac{A}{\gamma-1} \left(\frac{J}{\rho_0} \right)^{1-\gamma} + B \left(\frac{J}{\rho_0} \right). \quad (9)$$

For an *isentropic perfect gas* we have $B = 0$.

In our tests, we shall use the expression (8) for the treatment of an isentropic perfect gas, where the value of the constant $B \neq 0$ does not affect the dynamics, while it allows to naturally impose from (7) the boundary condition

$$P|_{\partial \mathcal{B}} = B,$$

with $P = A \left(\frac{\rho_0}{J} \right)^\gamma$ the pressure of the isentropic perfect gas. This is crucial for the discretization, since it allows to find the appropriate discretization of the boundary condition directly from the boundary terms of the discrete variational principle.

The *rotating shallow water model* can also be recasted in the formulation above, in which case the variable ρ_0 is interpreted as the water depth in the reference configuration. The Lagrangian is

$$L(\varphi, \dot{\varphi}, \nabla \varphi) = \frac{1}{2} \rho_0 |\dot{\varphi}|^2 + \rho_0 \dot{\varphi} \cdot R(\varphi) - \rho_0 W(\rho_0, J),$$

where R is the vector potential of the angular velocity of the Earth and W is chosen as

$$W(\rho_0, J) = g \frac{1}{2} \frac{\rho_0}{J}.$$

2.2 Incompressible fluid models

2.2.1 Hamilton principle with incompressibility constraint

Incompressible models are obtained by inserting the constraint $J = 1$ in the Hamilton principle as

$$\delta \int_0^T \int_{\mathcal{B}} (L(\varphi, \dot{\varphi}, \nabla \varphi) + \lambda(J - 1)) dt dX = 0, \quad (10)$$

where $\lambda(t, X)$ is the Lagrange multiplier. With the Lagrangian (4), this results in the system

$$\rho_0 \ddot{\varphi} + \frac{\partial}{\partial x^i} ((P_W + \lambda) J \mathbf{F}^{-1})^i = -\rho_0 \frac{\partial \Pi}{\partial \varphi}, \quad J = 1. \quad (11)$$

With the relations $\dot{\varphi} = u \circ \varphi$, $P_W = p_w \circ \varphi$, and $\rho_0 = (\rho \circ \varphi)J$, we get from (11) the familiar Eulerian formulation

$$\rho(\partial_t u + u \cdot \nabla u) = -\nabla(p_w + p_\lambda) - \rho \nabla \Pi, \quad \operatorname{div} u = 0, \quad \partial_t \rho + u \cdot \nabla \rho = 0.$$

In this case $p_w + p_\lambda$ is determined from the incompressibility constraint via a Poisson equation.

2.2.2 Example: Boussinesq model, nonhomogeneous Euler equations, and ideal fluid

The *Boussinesq model* is obtained from the Hamilton principle with incompressibility constraint (10) by interpreting ρ_0 as the buoyancy in the reference configuration and taking the Lagrangian

$$L(\varphi, \dot{\varphi}, \nabla \varphi) = \frac{1}{2} |\dot{\varphi}|^2 - \rho_0 \varphi \cdot \mathbf{g} \quad (12)$$

with gravitational acceleration vector \mathbf{g} . For the *nonhomogeneous Euler fluid*, the Lagrangian is the kinetic energy

$$L(\varphi, \dot{\varphi}, \nabla \varphi) = \frac{1}{2} \rho_0 |\dot{\varphi}|^2, \quad (13)$$

for some non-constant density $\rho_0(X)$. For the *ideal fluid*, one takes

$$L(\varphi, \dot{\varphi}, \nabla \varphi) = \frac{1}{2} |\dot{\varphi}|^2 \quad (14)$$

in (10), which gives

$$\ddot{\varphi} + \frac{\partial}{\partial x^i} (\lambda J \mathbf{F}^{-1})^i = 0, \quad J = 1, \quad (15)$$

and hence $\partial_t u + u \cdot \nabla u = -\nabla p_\lambda$, $\operatorname{div} u = 0$ is obtained in the Eulerian formulation.

2.3 Multisymplectic variational continuum mechanics

In this paragraph, we briefly review the geometric variational framework of classical field theory, as it applies to continuum mechanics, following [25]. This setting will be discretized in a structure preserving way which allows the identification of the notion of discrete multisymplecticity, discrete momentum map, and discrete Noether theorems.

2.3.1 Configuration bundle, jet bundle, and Lagrangian density

The geometric formulation of classical field theories starts with the identification of the configuration bundle of the theory, denoted $\pi_{\mathcal{Y},\mathcal{X}} : \mathcal{Y} \rightarrow \mathcal{X}$, such that the fields φ of the theory are sections of this fiber bundle, i.e., they are smooth maps $\varphi : \mathcal{X} \rightarrow \mathcal{Y}$ such that $\pi_{\mathcal{Y},\mathcal{X}} \circ \varphi = \text{id}_{\mathcal{X}}$, where $\text{id}_{\mathcal{X}}$ denotes the identity map on \mathcal{X} . We assume $\dim \mathcal{X} = n + 1$ and denote by x^μ , $\mu = 0, 1, 2, \dots, n$, the coordinates on \mathcal{X} . The fiber coordinates on \mathcal{Y} are y^a , $a = 1, \dots, N$, hence coordinates on the manifold \mathcal{Y} are (x^μ, y^a) , $\mu = 0, \dots, n$, $a = 1, \dots, N$. While the configuration bundle for continuum mechanics is a trivial bundle, it is advantageous to use the general setting of fiber bundles since it allows to efficiently particularise to continuum mechanics the intrinsic geometric formulation and structures of field theories.

The *first jet bundle* of the configuration bundle $\pi_{\mathcal{X},\mathcal{Y}} : \mathcal{Y} \rightarrow \mathcal{X}$ is the field theoretic analogue of the tangent bundle of classical mechanics, i.e., its fiber at y contains the first derivatives $\varphi^{a,\mu}(x)$ of a field φ at x with $\varphi(x) = y$. It is defined as the fiber bundle $\pi_{\mathcal{Y},J^1\mathcal{Y}} : J^1\mathcal{Y} \rightarrow \mathcal{Y}$ over \mathcal{Y} , whose fiber at $y \in \mathcal{Y}$ consists of linear maps $\gamma : T_x\mathcal{X} \rightarrow T_y\mathcal{Y}$ satisfying $T\pi_{\mathcal{Y},\mathcal{X}} \circ \gamma = \text{id}_{T_x\mathcal{X}}$, where $x = \pi_{\mathcal{X},\mathcal{Y}}(y)$. The induced coordinates on the fiber of $J^1\mathcal{Y} \rightarrow \mathcal{Y}$ are denoted v^a_μ . We note that $J^1\mathcal{Y}$ can also be regarded as the total space of a bundle over \mathcal{X} , namely $\pi_{\mathcal{X},J^1\mathcal{Y}} := \pi_{\mathcal{X},\mathcal{Y}} \circ \pi_{\mathcal{Y},J^1\mathcal{Y}} : J^1\mathcal{Y} \rightarrow \mathcal{X}$. Natural coordinates on the manifold $J^1\mathcal{Y}$ are hence (x^μ, y^a, v^a_μ) , $\mu = 0, \dots, n$, $a = 1, \dots, N$.

The derivative of a field φ can be regarded as a section of $\pi_{\mathcal{X},J^1\mathcal{Y}} : J^1\mathcal{Y} \rightarrow \mathcal{X}$, by writing $x \in \mathcal{X} \mapsto j^1\varphi(x) := T_x\varphi \in J^1_{\varphi(x)}\mathcal{Y}$, with $T_x\varphi : T_x\mathcal{X} \rightarrow T_{\varphi(x)}\mathcal{Y}$ the tangent map (or first derivative) of φ . The section $j^1\varphi$ is called the *first jet extension* of φ and is the intrinsic object corresponding to the value of a field and of its first derivatives, at the points in \mathcal{X} . In the natural coordinates (x^μ, y^a, v^a_μ) of $J^1\mathcal{Y}$, the first jet extension reads $j^1\varphi : x^\mu \mapsto (x^\mu, \varphi^a(x), \varphi^{a,\mu}(x))$.

A *Lagrangian density* is a smooth bundle map $\mathcal{L} : J^1\mathcal{Y} \rightarrow \Lambda^{n+1}\mathcal{X}$ over \mathcal{X} , where $\Lambda^{n+1}\mathcal{X} \rightarrow \mathcal{X}$ is the vector bundle of $(n + 1)$ -form on \mathcal{X} . In coordinates we write $\mathcal{L}(j^1\varphi(x)) = L(x^\mu, \varphi^a, \varphi^{a,\mu})d^{n+1}x$. The associated *action functional* is

$$S(\varphi) := \int_{\mathcal{X}} \mathcal{L}(j^1\varphi(x)). \quad (16)$$

2.3.2 The case of continuum mechanics

For continuum mechanics, the configuration bundle is the trivial fiber bundle

$$\mathcal{Y} = \mathcal{M} \times \mathcal{X} \rightarrow \mathcal{X}, \quad \text{with} \quad \mathcal{X} = \mathbb{R} \times \mathcal{B},$$

where \mathcal{B} is the reference configuration of the continuum and \mathcal{M} is the ambient space, see the beginning of §2. We have the equalities $x = (t, X)$ and $y = (x, m) = (t, X, m)$ between the variables of the general theory and those of continuum mechanics.

A section of this bundle is a map $\varphi : \mathcal{X} \rightarrow \mathcal{X} \times \mathcal{M}$, whose first component is $\text{id}_{\mathcal{X}}$. It is canonically identified with a map $\varphi : \mathcal{X} = \mathbb{R} \times \mathcal{B} \rightarrow \mathcal{M}$ referred to as the fluid configuration map above.

The first jet bundle is canonically identified with the vector bundle $L(T\mathcal{X}, T\mathcal{M}) \rightarrow \mathcal{Y} = \mathcal{X} \times \mathcal{M}$, whose fiber at $y = (x, m)$ is the vector space $L(T_x\mathcal{X}, T_m\mathcal{M})$ of linear maps from $T_x\mathcal{X}$ to $T_m\mathcal{M}$. The first jet extension is $j^1\varphi(t, X) = (\varphi(t, X), \dot{\varphi}(t, X), \nabla\varphi(t, X))$ and the Lagrangian density reads

$$\mathcal{L}(\varphi, \dot{\varphi}, \nabla\varphi) = L(\varphi, \dot{\varphi}, \nabla\varphi) dt \wedge d^n X$$

with L the Lagrangian of barotropic fluids given in (4).

2.3.3 Multisymplectic form and Cartan forms

Without entering into the details, we recall that the dual jet bundle $J^1\mathcal{Y}^* \rightarrow \mathcal{Y}$, defined as the bundle of affine maps $J^1\mathcal{Y} \rightarrow \Lambda^{n+1}\mathcal{X}$, is endowed with a *canonical* $(n+1)$ form Θ_{can} and a *canonical multisymplectic* $(n+2)$ -form $\Omega_{\text{can}} = -\mathbf{d}\Theta_{\text{can}}$. These are the field theoretic analogue to the canonical one-form and canonical symplectic form on the phase space (cotangent bundle of the configuration manifold) in classical mechanics. By pulling back these canonical forms with the Legendre transform $\mathbb{F}\mathcal{L} : J^1\mathcal{Y} \rightarrow J^1\mathcal{Y}^*$ of a given Lagrangian density $\mathcal{L} : J^1\mathcal{Y} \rightarrow \Lambda^{n+1}\mathcal{X}$, one gets the *Cartan forms* $\Theta_{\mathcal{L}}$ and $\Omega_{\mathcal{L}}$ on $J^1\mathcal{Y}$, see [18]. These forms appear naturally in the Hamilton principle, in the multisymplectic form formula, and in the Noether theorem, as will shall explain below. All these three notions have discrete analogues, that we shall deeply use in §3 and §4.

The Cartan forms arise in the Hamilton principle as follows. Using the relation $\mathcal{L}(j^1\varphi) = (j^1\varphi)^*\Theta_{\mathcal{L}}$, [18], the derivative of the action functional (16) takes the intrinsic form

$$\begin{aligned} \mathbf{d}S(\varphi) \cdot V(\varphi) &= \left. \frac{d}{d\varepsilon} \right|_{\varepsilon=0} \int_{\mathcal{X}} \mathcal{L}(j^1(\phi_\varepsilon \circ \varphi)) \\ &= - \int_{\mathcal{X}} (j^1\varphi)^* \mathbf{i}_{j^1V} \Omega_{\mathcal{L}} + \int_{\partial\mathcal{X}} (j^1\varphi)^* \mathbf{i}_{j^1V} \Theta_{\mathcal{L}}, \end{aligned} \quad (17)$$

where ϕ_ε is the flow of a vertical vector field V on \mathcal{Y} , i.e., $T\pi_{\mathcal{X},\mathcal{Y}} \circ V = 0$, and j^1V denotes the first jet extension of V to $J^1\mathcal{Y}$ defined as $j^1V = \left. \frac{d}{d\varepsilon} \right|_{\varepsilon=0} j^1\phi^\varepsilon$.

2.3.4 Multisymplectic form formula and Noether theorem

The multisymplectic form formula is a property of the solution of the Euler-Lagrange field equations that extends the symplectic property of the solution of the Euler-Lagrange equations of classical mechanics. It is obtained from the identity (17), by evaluating the action functional at a solution of the Euler-Lagrange equations and taking its derivative along variations of solutions, see [24]. Let φ be a solution of the Euler-Lagrange field equations and V, W solutions of the first variation of the Euler-Lagrange equations at φ . Then V, W, φ satisfy the *multisymplectic form formula*:

$$\int_{\partial U} (j^1\varphi)^* \mathbf{i}_{j^1V} \mathbf{i}_{j^1W} \Omega_{\mathcal{L}} = 0, \quad (18)$$

for all open subset $U \subset \mathcal{X}$ with with piecewise smooth boundary.

We now recall the general statement of the *covariant Noether theorem*. Let a Lie group G act on \mathcal{Y} and assume that the action covers a diffeomorphism of \mathcal{X} . Assume that the Lagrangian density \mathcal{L} is G -equivariant with respect to this action, see later in §3.1.7 for a concrete example. Then, considering only variations along the Lie group action, and restricting the action functional to an arbitrary open subset $U \subset \mathcal{X}$ with piecewise smooth boundary, formula (17) shows that a solution of the Euler-Lagrange field equations satisfy the *covariant Noether theorem*

$$\int_{\partial U} (j^1\varphi)^* J^{\mathcal{L}}(\xi) = 0, \quad \text{for all } \xi \in \mathfrak{g}, \quad (19)$$

where $J^{\mathcal{L}}(\xi) = \mathbf{i}_{j^1\xi_{\mathcal{Y}}} \Theta_{\mathcal{L}} : J^1\mathcal{Y} \rightarrow \mathfrak{g}^* \otimes \Lambda^n J^1\mathcal{Y}$ is the *covariant momentum map* associated to \mathcal{L} and $\xi_{\mathcal{Y}}$ is the infinitesimal generator of the Lie group action associated to the Lie algebra element $\xi \in \mathfrak{g}$.

3 2D Discrete barotropic and incompressible fluid models

In this section we propose a multisymplectic variational discretization of fluid mechanics, by focusing on compressible barotropic models and incompressible models. We consider free boundary fluids, as well as fluid impacting on a surface. A main step in our construction is the definition of discrete deformation gradient and discrete Jacobian.

3.1 Multisymplectic discretizations

We consider the geometric setting of continuum mechanics with the configuration bundle $\mathcal{Y} = \mathcal{X} \times \mathcal{M} \rightarrow \mathcal{X} = \mathbb{R} \times \mathcal{B}$. We assume that \mathcal{B} is a rectangle in \mathbb{R}^2 and take $\mathcal{M} = \mathbb{R}^2$.

3.1.1 Discrete configuration bundle

The general discrete setting is the following. One first considers a *discrete parameter space* \mathcal{U}_d and a *discrete base-space configuration*, which is a one-to-one map

$$\phi_{\mathcal{X}_d} : \mathcal{U}_d \rightarrow \phi_{\mathcal{X}_d}(\mathcal{U}_d) = \mathcal{X}_d \subset \mathcal{X}$$

whose image is the discrete spacetime \mathcal{X}_d . The *discrete configuration bundle* is defined as $\pi_d : \mathcal{Y}_d = \mathcal{X}_d \times \mathcal{M} \rightarrow \mathcal{X}_d$. The *discrete fields* are the sections of the discrete configuration bundle, identified with maps $\varphi_d : \mathcal{X}_d \rightarrow \mathcal{M}$. In order to describe both the discrete spacetime as well as the discrete field, one introduces the *discrete configuration* $\phi_d : \mathcal{U}_d \rightarrow \mathcal{Y}$, from which the discrete base-space configuration and the discrete physical deformation are obtained as $\phi_{\mathcal{X}_d} = \pi_d \circ \phi_d$ and $\varphi_d = \phi_d \circ \phi_{\mathcal{X}_d}^{-1}$, see Fig. 1. This setting is particularly well adapted to situations where the discrete spacetime is also variable, see [21, 9].

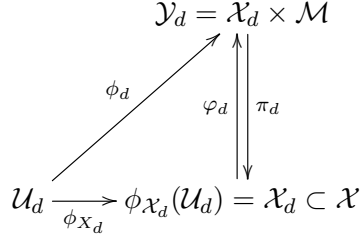


Figure 1: Discrete configuration and discrete configuration bundle

We consider the discrete parameter space defined by $\mathcal{U}_d := \{0, \dots, j, \dots, N\} \times \mathbb{B}_d$, where $\{0, \dots, j, \dots, N\}$ encodes an increasing sequence of time and \mathbb{B}_d parameterizes the nodes and simplexes of the discretization of \mathcal{B} . In this paper we restrict to the case $\mathbb{B}_d = \{0, \dots, A\} \times \{0, \dots, B\}$, where A and B are the number of spatial grid points. Therefore, $\mathcal{U}_d = \{0, \dots, N\} \times \{0, \dots, A\} \times \{0, \dots, B\}$ with elements denoted $(j, a, b) \in \mathcal{U}_d$. The discrete parameter space determines a set of parallelepipeds, denoted $\square_{a,b}^j$, and defined by the following eight pairs of indices (see Fig. 2)

$$\square_{a,b}^j = \{(j, a, b), (j+1, a, b), (j, a+1, b), (j, a, b+1), (j, a+1, b+1), (j+1, a+1, b), (j+1, a, b+1), (j+1, a+1, b+1)\}, \quad (20)$$

$j = 0, \dots, N-1, a = 0, \dots, A-1, b = 0, \dots, B-1$. The set of all such parallelepipeds is denoted \mathcal{U}_d^{\square} .

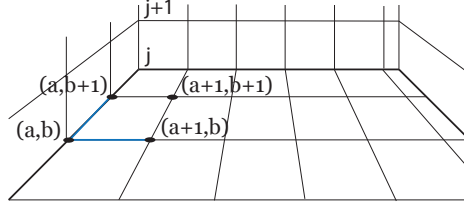


Figure 2: Discrete spacetime domain \mathcal{U}_d .

3.1.2 Discrete Jacobian

As recalled above, in the continuous setting, the material internal energy function $W(\rho_0, J)$ of the barotropic fluid depends on the deformation gradient only through its Jacobian. To define the discrete deformation gradient and the discrete Jacobian, we assume that the discrete base space configuration is of the form

$$\phi_{\mathcal{X}_d}(j, a, b) = s_{a,b}^j = (t^j, z_a^j, z_b^j) \in \mathbb{R} \times \mathcal{B}, \quad (21)$$

see Fig. 3. The discrete field φ_d evaluated at $s_{a,b}^j$ is denoted $\varphi_{a,b}^j := \varphi_d(s_{a,b}^j)$, see Fig. 4.

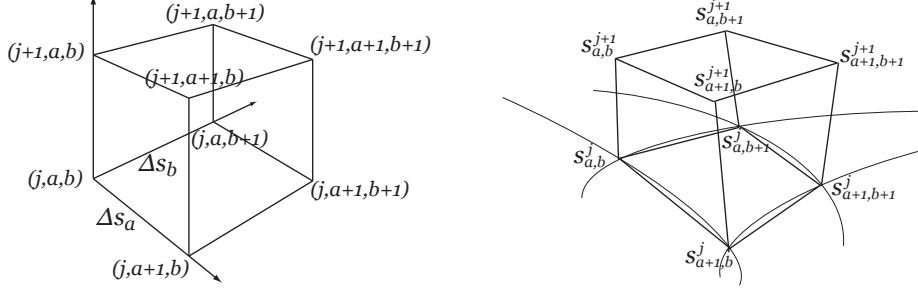


Figure 3: On the left: discrete coordinate system. On the right: Nodes of the mesh with Euclidean coordinates.

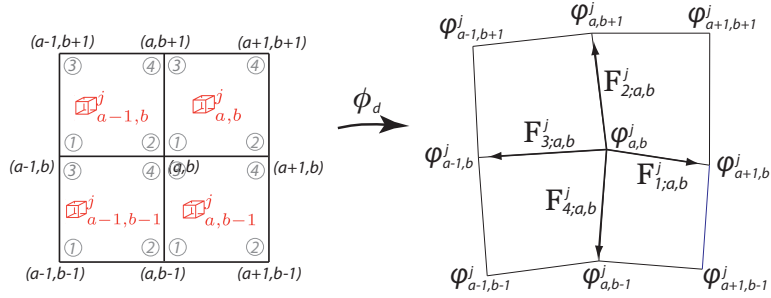


Figure 4: Discrete field $\phi_d = \varphi_d \circ \phi_{\mathcal{X}_d}$ evaluated on $\mathbb{P}_{a,b}^j, \mathbb{P}_{a,b}^j, \mathbb{P}_{a,b}^j, \mathbb{P}_{a,b}^j$ at time t^j .

Given a discrete base space configuration $\phi_{\mathcal{X}_d}$ and a discrete field φ_d , we define the following four vectors $\mathbf{F}_{\ell;a,b}^j \in \mathbb{R}^2$, $\ell = 1, 2, 3, 4$ at each node $(j, a, b) \in \mathcal{U}_d$, see Fig. 4 on the right:

$$\mathbf{F}_{1;a,b}^j = \frac{\varphi_{a+1,b}^j - \varphi_{a,b}^j}{|s_{a+1,b}^j - s_{a,b}^j|} \quad \text{and} \quad \mathbf{F}_{2;a,b}^j = \frac{\varphi_{a,b+1}^j - \varphi_{a,b}^j}{|s_{a,b+1}^j - s_{a,b}^j|} \quad (22)$$

$$\mathbf{F}_{3;a,b}^j = \frac{\varphi_{a-1,b}^j - \varphi_{a,b}^j}{|s_{a,b}^j - s_{a-1,b}^j|} = -\mathbf{F}_{1;a-1,b}^j \quad \text{and} \quad \mathbf{F}_{4;a,b}^j = \frac{\varphi_{a,b-1}^j - \varphi_{a,b}^j}{|s_{a,b}^j - s_{a,b-1}^j|} = -\mathbf{F}_{2;a,b-1}^j.$$

Based on these definitions, the discrete gradient is constructed as follows.

Definition 3.1 The discrete gradient deformations of a discrete field φ_d at the parallelepiped $\mathbb{P}_{a,b}^j$ are the four 2×2 matrices $\mathbf{F}^\ell(\mathbb{P}_{a,b}^j)$, $\ell = 1, 2, 3, 4$, defined at the four nodes at time t^j of $\mathbb{P}_{a,b}^j$, as follows:

$$\mathbf{F}_1(\mathbb{P}_{a,b}^j) = \begin{bmatrix} \mathbf{F}_{1;a,b}^j & \mathbf{F}_{2;a,b}^j \end{bmatrix}, \quad \mathbf{F}_2(\mathbb{P}_{a,b}^j) = \begin{bmatrix} \mathbf{F}_{2;a+1,b}^j & \mathbf{F}_{3;a+1,b}^j \end{bmatrix}, \quad (23)$$

$$\mathbf{F}_3(\mathbb{P}_{a,b}^j) = \begin{bmatrix} \mathbf{F}_{4;a,b+1}^j & \mathbf{F}_{1;a,b+1}^j \end{bmatrix}, \quad \mathbf{F}_4(\mathbb{P}_{a,b}^j) = \begin{bmatrix} \mathbf{F}_{3;a+1,b+1}^j & \mathbf{F}_{4;a+1,b+1}^j \end{bmatrix}.$$

The ordering $\ell = 1$ to $\ell = 4$ is respectively associated to the nodes (j, a, b) , $(j, a, b + 1)$, $(j, a + 1, b)$, $(j, a + 1, b + 1)$, see Fig. 4 on the left.

It is assumed that the discrete field φ_d is such that the determinant of the discrete gradient deformations are positive.

Definition 3.2 *The discrete Jacobians of a discrete field φ_d at the parallelepiped $\mathbb{P}_{a,b}^j$ are the four numbers $J_\ell(\mathbb{P}_{a,b}^j)$, $\ell = 1, 2, 3, 4$, defined at the four nodes at time t^j of $\mathbb{P}_{a,b}^j$ as follows:*

$$\begin{aligned} J_1(\mathbb{P}_{a,b}^j) &= |\mathbf{F}_{1;a,b}^j \times \mathbf{F}_{2;a,b}^j| = \det(\mathbf{F}_1(\mathbb{P}_{a,b}^j)), \\ J_2(\mathbb{P}_{a,b}^j) &= |\mathbf{F}_{2;a+1,b}^j \times \mathbf{F}_{3;a+1,b}^j| = \det(\mathbf{F}_2(\mathbb{P}_{a,b}^j)) \\ J_3(\mathbb{P}_{a,b}^j) &= |\mathbf{F}_{4;a,b+1}^j \times \mathbf{F}_{1;a,b+1}^j| = \det(\mathbf{F}_3(\mathbb{P}_{a,b}^j)) \\ J_4(\mathbb{P}_{a,b}^j) &= |\mathbf{F}_{3;a+1,b+1}^j \times \mathbf{F}_{4;a+1,b+1}^j| = \det(\mathbf{F}_4(\mathbb{P}_{a,b}^j)). \end{aligned} \tag{24}$$

As a consequence, from relations (24), the variation of the discrete Jacobian is given by

$$\delta J_\ell = \frac{\partial \det(\mathbf{F}_\ell)}{\partial \mathbf{F}_\ell} : \delta \mathbf{F}_\ell = J_\ell(\mathbf{F}_\ell)^{-\top} : \delta \mathbf{F}_\ell,$$

at each $\mathbb{P}_{a,b}^j$, which is used in the derivation of the discrete Euler-Lagrange equations.

3.1.3 Discrete Lagrangian

Recall that the set of all parallelepipeds in the discrete parameter space is denoted $\mathcal{U}_d^{\mathbb{P}}$. We write

$$\mathcal{X}_d^{\mathbb{P}} := \phi_{\mathcal{X}_d}(\mathcal{U}_d^{\mathbb{P}})$$

the set of all parallelepipeds in \mathcal{X}_d . The *discrete version of the first jet bundle* is given by

$$J^1 \mathcal{Y}_d := \mathcal{X}_d^{\mathbb{P}} \times \underbrace{\mathcal{M} \times \dots \times \mathcal{M}}_{8 \text{ times}} \rightarrow \mathcal{X}_d^{\mathbb{P}}. \tag{25}$$

Given a discrete field φ_d , its *first jet extension* is the section of (25) defined by

$$j^1 \varphi_d(\mathbb{P}_{a,b}^j) = (\varphi_{a,b}^j, \varphi_{a,b}^{j+1}, \varphi_{a+1,b}^j, \varphi_{a+1,b}^{j+1}, \varphi_{a,b+1}^j, \varphi_{a,b+1}^{j+1}, \varphi_{a+1,b+1}^j, \varphi_{a+1,b+1}^{j+1}), \tag{26}$$

which associates to each parallelepiped, the values of the field at its nodes. A *discrete Lagrangian* is a map

$$\mathcal{L}_d : J^1 \mathcal{Y}_d \rightarrow \mathbb{R},$$

see [24]. The discrete Lagrangian evaluated on a discrete field is denoted as

$$\mathcal{L}_d(j^1 \varphi_d(\mathbb{P})).$$

We now consider the case of the barotropic fluid. We assume for simplicity that the mass density ρ_0 of the fluid in the reference configuration is a constant number. The case of a Lagrangian density with a nonconstant mass density ρ_0 is important for

applications to stratified flows and can be easily treated by our approach. We consider a class of discrete Lagrangians associated to (4) of the form

$$\mathcal{L}_d(j^1\varphi_d(\mathbb{D})) = \text{vol}(\mathbb{D}) \left(\rho_0 K_d(j^1\varphi_d(\mathbb{D})) - \rho_0 W_d(\rho_0, j^1\varphi_d(\mathbb{D})) - \rho_0 \Pi_d(j^1\varphi_d(\mathbb{D})) \right), \quad (27)$$

where $\text{vol}(\mathbb{D})$ is the volume of the parallelepiped $\mathbb{D} \in \mathcal{X}_d^{\mathbb{D}}$. Examples of K_d, W_d, Π_d are given as follows.

- The discrete kinetic energy $K_d : J^1\mathcal{Y}_d \rightarrow \mathbb{R}$ is defined as

$$K_d(j^1\varphi_d(\mathbb{D}_{a,b}^j)) := \frac{1}{4} \sum_{\alpha=a}^{a+1} \sum_{\beta=b}^{b+1} \frac{1}{2} |v_{\alpha,\beta}^j|^2, \quad (28)$$

with $v_{\alpha,\beta}^j = (\varphi_{\alpha,\beta}^{j+1} - \varphi_{\alpha,\beta}^j) / \Delta t^j$ the discrete velocity.

- The discrete internal energy $W_d : J^1\mathcal{Y}_d \rightarrow \mathbb{R}$ is defined as

$$W_d(\rho_0, j^1\varphi_d(\mathbb{D}_{a,b}^j)) := \frac{1}{4} \sum_{\ell=1}^4 W(\rho_0, J_\ell(\mathbb{D}_{a,b}^j)), \quad (29)$$

where W is the material internal energy of the continuous model and $J_\ell(\mathbb{D}_{a,b}^j)$ are the discrete Jacobians associated to $\mathbb{D}_{a,b}^j$ at time t^j .

- The discrete potential energy $\Pi_d : J^1\mathcal{Y}_d \rightarrow \mathbb{R}$ is given by

$$\Pi_d(j^1\varphi_d(\mathbb{D}_{a,b}^j)) := \frac{1}{4} \sum_{\alpha=a}^{a+1} \sum_{\beta=b}^{b+1} \Pi(\varphi_{\alpha,\beta}^j), \quad (30)$$

where Π is the potential energy of the continuous model. We shall focus on the gravitation potential $\Pi(\varphi) = \mathbf{g} \cdot \varphi$, with gravitational acceleration vector \mathbf{g} , in which case

$$\Pi_d(j^1\varphi_d(\mathbb{D}_{a,b}^j)) = \frac{1}{4} \sum_{\alpha=a}^{a+1} \sum_{\beta=b}^{b+1} \mathbf{g} \cdot \varphi_{\alpha,\beta}^j. \quad (31)$$

We will also consider a mid-point rule discretization later in §3.2.1.

3.1.4 Discrete variations and discrete Euler-Lagrange equations

To simplify the exposition, we assume that the discrete base space configuration is fixed and given by $\phi_{\mathcal{X}_d}(j, a, b) = (j\Delta t, a\Delta s_1, b\Delta s_2)$, for given $\Delta t, \Delta s_1, \Delta s_2$, that is, we assume that the mesh is fixed¹ and matches with the standard basis axis of the Euclidean space

¹Mesh deformations can be also considered in this setting and will be explored in a future work.

(reference frame). In this case, we have $\text{vol}(\mathbb{D}) = \Delta t \Delta s_1 \Delta s_2$ in the discrete Lagrangian (27) and the mass of each $2D$ cell in $\phi_{\mathcal{X}_d}(\mathbb{B}_d)$ is $M = \rho_0 \Delta s_1 \Delta s_2$.

The discrete action functional associated to \mathcal{L}_d is obtained as

$$S_d(\varphi_d) = \sum_{\mathbb{D} \in \mathcal{X}_d^{\mathbb{D}}} \mathcal{L}_d(j^1 \varphi_d(\mathbb{D})) = \sum_{j=0}^{N-1} \sum_{a=0}^{A-1} \sum_{b=0}^{B-1} \mathcal{L}_d(j^1 \varphi_d(\mathbb{D}_{a,b}^j)). \quad (32)$$

In order to apply the discrete Hamilton principle, we compute the variation $\delta S_d(\varphi_d)$ of the action sum and we get

$$\begin{aligned} \sum_{j=0}^{N-1} \sum_{a=0}^{A-1} \sum_{b=0}^{B-1} \left[\frac{M}{4} \left(v_{a,b}^j \cdot \delta \varphi_{a,b}^{j+1} + v_{a+1,b}^j \cdot \delta \varphi_{a+1,b}^{j+1} + v_{a,b+1}^j \cdot \delta \varphi_{a,b+1}^{j+1} + v_{a+1,b+1}^j \cdot \delta \varphi_{a+1,b+1}^{j+1} \right) \right. \\ \left. + A_{a,b}^j \cdot \delta \varphi_{a,b}^j + B_{a,b}^j \cdot \delta \varphi_{a+1,b}^j + C_{a,b}^j \cdot \delta \varphi_{a,b+1}^j + D_{a,b}^j \cdot \delta \varphi_{a+1,b+1}^j \right], \end{aligned}$$

where we have used the following expressions of the partial derivative of \mathcal{L}_d :

$$\begin{aligned} D_2 \mathcal{L}_{a,b}^j &= \frac{M}{4} v_{a,b}^j & D_6 \mathcal{L}_{a,b}^j &= \frac{M}{4} v_{a,b+1}^j \\ D_4 \mathcal{L}_{a,b}^j &= \frac{M}{4} v_{a+1,b}^j & D_8 \mathcal{L}_{a,b}^j &= \frac{M}{4} v_{a+1,b+1}^j \end{aligned} \quad (33)$$

and we have introduced the following notations for the other partial derivatives

$$\begin{aligned} D_1 \mathcal{L}_{a,b}^j &= A_{a,b}^j & D_5 \mathcal{L}_{a,b}^j &= C_{a,b}^j \\ D_3 \mathcal{L}_{a,b}^j &= B_{a,b}^j & D_7 \mathcal{L}_{a,b}^j &= D_{a,b}^j, \end{aligned} \quad (34)$$

whose expressions are given in Appendix A.1 for an arbitrary internal energy function W . Note that $D_k \mathcal{L}_{a,b}^j$ is the partial derivative of \mathcal{L}_d , at $\mathbb{D}_{a,b}^j$, with respect to the k^{th} variable, in the order listed in (26).

Rearranging the expression (33) we get the discrete Euler-Lagrange equations

$$M v_{a,b}^{j-1} + A_{a,b}^j + B_{a-1,b}^j + C_{a,b-1}^j + D_{a-1,b-1}^j = 0, \quad (35)$$

which correspond to variations $\delta \varphi_{a,b}^j$ at the interior of the domain. Variations at the spatial boundary gives the boundary conditions

$$\begin{cases} \frac{M}{2} v_{0,b}^{j-1} + A_{0,b}^j + C_{0,b-1}^j = 0, & \frac{M}{2} v_{a,0}^{j-1} + A_{a,0}^j + B_{a-1,0}^j = 0, \\ \frac{M}{2} v_{A,b}^{j-1} + B_{A-1,b}^j + D_{A-1,b-1}^j = 0, & \frac{M}{2} v_{a,B}^{j-1} + C_{a,B-1}^j + D_{a-1,B-1}^j = 0, \\ \frac{M}{4} v_{0,0}^{j-1} + A_{0,0}^j = 0, & \frac{M}{4} v_{A,0}^{j-1} + B_{A-1,0}^j = 0, \\ \frac{M}{4} v_{0,B}^{j-1} + C_{0,B-1}^j = 0, & \frac{M}{4} v_{A,B}^{j-1} + D_{A-1,B-1}^j = 0, \end{cases} \quad (36)$$

while variations at the temporal boundary gives

$$\begin{cases} A_{a,b}^0 + B_{a-1,b}^0 + C_{a,b-1}^0 + D_{a-1,b-1}^0 = 0, & Mv_{a,b}^{N-1} = 0, \\ A_{0,b}^0 + C_{0,b-1}^0 = 0, & A_{a,0}^0 + B_{a-1,0}^0 = 0, \\ B_{A-1,b}^0 + D_{A-1,b-1}^0 = 0, & C_{a,B-1}^0 + D_{a-1,B-1}^0 = 0. \end{cases} \quad (37)$$

We assume that the variations of the discrete field at the spatial boundary are arbitrary so we get the boundary conditions (36). This corresponds to the discrete version of the boundary condition (6). We assume that the variations at the temporal extremity vanish, hence (37) is not imposed.

3.1.5 Discrete Cartan forms

In a similar way with the continuous case recalled in §2.3, the discrete multisymplectic form formula and the discrete Noether theorem are efficiently derived and written by using discrete analogues to the Cartan forms $\Theta_{\mathcal{L}}$ and $\Omega_{\mathcal{L}}$ on the first jet bundle $J^1\mathcal{Y}$, see §2.3.3, and by using differential exterior calculus. The discrete Cartan forms of multisymplectic variational integrators are the natural spacetime generalizations of the discrete Cartan forms appearing in time variational integrators, [26].

Given a discrete Lagrangian $\mathcal{L}_d : J^1\mathcal{Y}_d \rightarrow \mathbb{R}$, the *discrete Cartan one-forms* are defined on the discrete first jet bundle (25) as

$$\Theta_{\mathcal{L}_d}^{\mathfrak{p}} = D_{\mathfrak{p}}\mathcal{L}_d d\varphi_d^{(\mathfrak{p})}, \quad \mathfrak{p} = 1, \dots, 8, \quad (38)$$

see [24, 21, 9]. In (38) we have used the notation

$$\varphi_d^{(\mathfrak{p})} \in \{\varphi_{a,b}^j, \varphi_{a,b}^{j+1}, \varphi_{a+1,b}^j, \varphi_{a+1,b}^{j+1}, \varphi_{a,b+1}^j, \varphi_{a,b+1}^{j+1}, \varphi_{a+1,b+1}^j, \varphi_{a+1,b+1}^{j+1}\}. \quad (39)$$

For the discrete Lagrangian (27) of the barotropic fluid, using (34) and (33) we get the following expressions of the discrete Cartan one-forms evaluated on the first jet extension $j^1\varphi_d(\mathbb{E}_{a,b}^j) \in J^1\mathcal{Y}_d$ of discrete field φ_d :

$$\begin{aligned} \Theta_{\mathcal{L}_d}^1 &= A_{a,b}^j d\varphi_{a,b}^j, & \Theta_{\mathcal{L}_d}^2 &= \frac{M}{4} v_{a,b}^j d\varphi_{a,b}^{j+1}, \\ \Theta_{\mathcal{L}_d}^3 &= B_{a,b}^j d\varphi_{a+1,b}^j, & \Theta_{\mathcal{L}_d}^4 &= \frac{M}{4} v_{a+1,b}^j d\varphi_{a+1,b}^{j+1}, \\ \Theta_{\mathcal{L}_d}^5 &= C_{a,b}^j d\varphi_{a,b+1}^j, & \Theta_{\mathcal{L}_d}^6 &= \frac{M}{4} v_{a,b+1}^{j+1} d\varphi_{a,b+1}^{j+1}, \\ \Theta_{\mathcal{L}_d}^7 &= D_{a,b}^j d\varphi_{a+1,b+1}^j, & \Theta_{\mathcal{L}_d}^8 &= \frac{M}{4} v_{a+1,b+1}^j d\varphi_{a+1,b+1}^{j+1}. \end{aligned} \quad (40)$$

In order to present the multisymplectic form formula and the discrete covariant Noether theorem, we shall rewrite the differential of the discrete action functional (32) in an intrinsic form using the discrete Cartan one-forms. Given a vector field V_d tangent

to the discrete configuration φ_d , we consider its first jet extension j^1V_d which attributes to the set of nodes in \mathbb{D} the set of values of V_d on these nodes. With this definition, for a given $\mathbb{D} \in \mathcal{X}_d^{\mathbb{D}}$, we can write the partial derivatives of \mathcal{L}_d in terms of the discrete Cartan forms as

$$D_{\mathbf{p}}\mathcal{L}_d(j^1\varphi_d(\mathbb{D})) \cdot V_d^{(\mathbf{p})} = \Theta_{\mathcal{L}_d}^{\mathbf{p}}(j^1\varphi_d(\mathbb{D})) \cdot j^1V_d = \left[(j^1\varphi_d)^* (\mathbf{i}_{j^1V_d} \Theta_{\mathcal{L}_d}^{\mathbf{p}}) \right] (\mathbb{D}), \quad (41)$$

for $\mathbf{p} = 1, \dots, 8$. In the last term we have used standard notations from differential calculus: the notation $(j^1\varphi)^*$ for the pull-back by $j^1\varphi$ of k -forms from $J^1\mathcal{Y}_d$ to $\mathcal{X}_d^{\mathbb{D}}$ and the notation $\mathbf{i}_{j^1V_d}$ for the insertion of a vector in a k -form. With these notations, the total derivative of the discrete action functional (32) is

$$\mathbf{d}S_d(\varphi_d) \cdot V_d = \sum_{\mathbb{D} \in \mathcal{U}_d^{\mathbb{D}}} \sum_{\mathbf{p} \in \mathbb{D}} \left[(j^1\varphi_d)^* (\mathbf{i}_{j^1V_d} \Theta_{\mathcal{L}_d}^{\mathbf{p}}) \right] (\mathbb{D}). \quad (42)$$

Here $\mathbf{p} \in \mathbb{D}$ denotes a node \mathbf{p} of the parallelepiped \mathbb{D} . Such a formula is true on any subdomain $\mathcal{U}'_d \subset \mathcal{U}_d$, by considering the restricted action $S'_d = S_d|_{\mathcal{U}'_d}$.

3.1.6 Discrete multisymplectic form formula and discrete Noether theorem

When restricted to a solution φ_d of (35), the total derivative of S_d reads

$$\mathbf{d}S_d(\varphi_d) \cdot V_d = \sum_{\mathbb{D} \in \mathcal{U}_d^{\mathbb{D}}} \sum_{\mathbf{p}; \mathbb{D}^{(\mathbf{p})} \in \partial\mathcal{U}_d} \left[(j^1\varphi_d)^* (\mathbf{i}_{j^1V_d} \Theta_{\mathcal{L}_d}^{\mathbf{p}}) \right] (\mathbb{D}), \quad (43)$$

similarly on any subdomains $\mathcal{U}'_d \subset \mathcal{U}_d$. Note the difference with formula (42). From (43) two important results are obtained:

1. The *discrete multisymplectic form formula*.

It is obtained by taking the exterior derivative of (43), evaluating it on the first variations V_d, W_d of a solution φ_d , and using the rules of exterior differential calculus, which gives

$$\mathbf{d}\mathbf{d}S_d(\varphi_d)(V_d, W_d) = \sum_{\mathbb{D} \in \mathcal{U}'_d} \sum_{\mathbf{p}; \mathbb{D}^{(\mathbf{p})} \in \partial\mathcal{U}'_d} \left[(j^1\varphi_d)^* (\mathbf{i}_{j^1V_d} \mathbf{i}_{j^1W_d} \Omega_{\mathcal{L}_d}^{\mathbf{p}}) \right] (\mathbb{D}) = 0, \quad (44)$$

for any subdomains $\mathcal{U}'_d \subset \mathcal{U}_d$. Here $\Omega_{\mathcal{L}_d}^{\mathbf{p}} = -\mathbf{d}\Theta_{\mathcal{L}_d}^{\mathbf{p}}$, $\mathbf{p} = 1, \dots, 8$ are the *discrete Cartan 2-forms* on $J^1\mathcal{Y}_d$, see [24]. This is the discrete version of the multisymplectic form formula (18). It extends to spacetime discretization, the symplectic property of variational integrators, [26]. This formula encodes a discrete version of the reciprocity theorem of continuum mechanics, as well as discrete time symplecticity of the solution flow, see [21].

2. The *discrete covariant Noether theorem*.

Consider an action $\Phi : G \times \mathcal{M} \rightarrow \mathcal{M}$ of a Lie group G on \mathcal{M} . For $\xi \in \mathfrak{g}$, the Lie algebra of G , we denote by $\xi_{\mathcal{M}}$ the infinitesimal generator of the action, i.e. the vector field on \mathcal{M} defined by

$$\xi_{\mathcal{M}}(m) := \left. \frac{d}{d\varepsilon} \right|_{\varepsilon=0} \Phi_{\exp(\varepsilon\xi)}(m),$$

for every $m \in \mathcal{M}$. Assume that \mathcal{L}_d is G -invariant with respect this action. As a consequence, the discrete action is also G -invariant and we get

$$\mathbf{d}S'_d(\varphi_d) \cdot \xi_{\mathcal{M}}(\varphi_d) = 0 \quad \text{for all } \xi \in \mathfrak{g}. \quad (45)$$

From (43), it follows

$$\mathbf{d}S'_d(\varphi_d) \cdot \xi_{\mathcal{M}}(\varphi_d) = \sum_{\mathbb{D} \in \mathcal{U}'_d} \sum_{\mathbf{p}; \mathbb{D}^{(\mathbf{p})} \in \partial\mathcal{U}'_d} \left[(j^1\varphi_d)^* \langle J_{\mathcal{L}_d}^{\mathbf{p}}, \xi \rangle \right] (\mathbb{D}) = 0, \quad (46)$$

for every $\xi \in \mathfrak{g}$, where the *discrete covariant momentum maps* are defined by

$$J_{\mathcal{L}_d}^{\mathbf{p}} : J^1\mathcal{Y}_d \rightarrow \mathfrak{g}^*, \quad \langle J_{\mathcal{L}_d}^{\mathbf{p}}, \xi \rangle := \mathbf{i}_{\xi_{J^1\mathcal{Y}_d}} \Theta_{\mathcal{L}_d}^{\mathbf{p}}, \quad \xi \in \mathfrak{g}, \quad \mathbf{p} = 1, \dots, 8. \quad (47)$$

In (47) $\xi_{J^1\mathcal{Y}_d}$ is the infinitesimal generator of the action of G induced on $J^1\mathcal{Y}_d$ by the action Φ on \mathcal{M} . It is given at each $j^1\varphi_d(\mathbb{D}_{a,b}^j) \in J^1\mathcal{Y}_d$ by

$$\begin{aligned} \xi_{J^1\mathcal{Y}_d}(j^1\varphi_d(\mathbb{D}_{a,b}^j)) &= \left(\mathbb{D}_{a,b}^j, \xi_{\mathcal{M}}(\varphi_{a,b}^j), \xi_{\mathcal{M}}(\varphi_{a,b}^{j+1}), \xi_{\mathcal{M}}(\varphi_{a+1,b}^j), \xi_{\mathcal{M}}(\varphi_{a+1,b}^{j+1}), \right. \\ &\quad \left. \xi_{\mathcal{M}}(\varphi_{a,b+1}^j), \xi_{\mathcal{M}}(\varphi_{a,b+1}^{j+1}), \xi_{\mathcal{M}}(\varphi_{a+1,b+1}^j), \xi_{\mathcal{M}}(\varphi_{a+1,b+1}^{j+1}) \right). \end{aligned}$$

From (46), we thus obtain the *discrete covariant Noether theorem*

$$\sum_{\mathbb{D} \in \mathcal{U}'_d} \sum_{\mathbf{p}; \mathbb{D}^{(\mathbf{p})} \in \partial\mathcal{U}'_d} J_{\mathcal{L}_d}^{\mathbf{p}}(\mathbb{D}) = 0, \quad (48)$$

for every subdomain $\mathcal{U}'_d \subset \mathcal{U}_d$ and for φ_d a solution of the discrete Euler-Lagrange equations. This is the discrete version of the covariant Noether theorem (19).

We refer to [21], [8], [9] for more explanations concerning discrete conservation laws for multisymplectic variational discretizations.

3.1.7 Symmetries for barotropic fluids

In absence of the gravitation potential, the discrete Lagrangian (27) is invariant under rotation and translation, i.e., the action of the special Euclidean group $SE(2)$. This follows from inspection of the expressions (28) and (29), and the expression of the discrete Jacobian.

From this invariance, the discrete covariant Noether theorem (48) is satisfied with the discrete covariant momentum maps $J_{\mathcal{L}_d}^{\mathfrak{p}} : J^1\mathcal{Y}_d \rightarrow \mathfrak{se}(2)^*$ given by

$$J_{\mathcal{L}_d}^{\mathfrak{p}}(j^1\varphi_d(\mathbb{P}_{a,b}^j)) = (\varphi^{(\mathfrak{p})} \times D_{\mathfrak{p}}\mathcal{L}_{a,b}^j, D_{\mathfrak{p}}\mathcal{L}_{a,b}^j), \quad \mathfrak{p} = 1, \dots, 8. \quad (49)$$

A consequence of this discrete covariant Noether theorem is the conservation of the *classical* discrete momentum map given in terms of the discrete *covariant* momentum map as

$$\begin{aligned} \mathbf{J}_d^j = \mathbf{J}_d(\varphi^j, \varphi^{j+1}) &= \sum_{a=0}^{A-1} \sum_{b=0}^{B-1} (J_{\mathcal{L}_d}^2 + J_{\mathcal{L}_d}^4 + J_{\mathcal{L}_d}^6 + J_{\mathcal{L}_d}^8) \\ &= - \sum_{a=0}^{A-1} \sum_{b=0}^{B-1} (J_{\mathcal{L}_d}^1 + J_{\mathcal{L}_d}^3 + J_{\mathcal{L}_d}^5 + J_{\mathcal{L}_d}^7), \end{aligned} \quad (50)$$

i.e., $\mathbf{J}_d^{j+1} = \mathbf{J}_d^j$. On the left hand side $\varphi^j = \{\varphi_{a,b}^j \mid 0 \leq a \leq A-1, 0 \leq b \leq B-1\}$ is the collection of all positions at time t^j . On the right hand sides each of the discrete momentum maps $J_{\mathcal{L}_d}^{\mathfrak{p}}$ are evaluated on $j^1\varphi_d(\mathbb{P}_{a,b}^j)$. We refer to [8] for details regarding the link between discrete *classical* and discrete *covariant* momentum maps underlying formulas like (50). Boundary conditions play an important role in this correspondence.

From (49), (50), and Appendix A.1, we get the expression

$$\mathbf{J}_d^j = \begin{bmatrix} \sum_{a=0}^{A-1} \sum_{b=0}^{B-1} \mathbf{J}_r(j^1\varphi_d(\mathbb{P}_{a,b}^j)) \\ \sum_{a=0}^{A-1} \sum_{b=0}^{B-1} \mathbf{J}_l(j^1\varphi_d(\mathbb{P}_{a,b}^j)) \end{bmatrix} \quad \text{with} \quad \begin{aligned} \mathbf{J}_r(j^1\varphi_d(\mathbb{P}_{a,b}^j)) &= \sum_{\alpha=a}^{a+1} \sum_{\beta=b}^{b+1} \varphi_{\alpha,\beta}^j \times \frac{M}{4} v_{\alpha,\beta}^j \in \mathbb{R}, \\ \mathbf{J}_l(j^1\varphi_d(\mathbb{P}_{a,b}^j)) &= \sum_{\alpha=a}^{a+1} \sum_{\beta=b}^{b+1} \frac{M}{4} v_{\alpha,\beta}^j \in \mathbb{R}^2. \end{aligned} \quad (51)$$

3.2 Incompressible models and penalty method

In this section we adapt the multisymplectic variational integrator obtained above to the case of incompressible models.

Equality constraint. As recalled in §2.2.1, incompressible models can be obtained from a Lagrange multiplier approach which imposes the equality constraint $J = 1$. In the discrete case, one similarly adds to the discrete action (32) the corresponding Lagrange multiplier term to get

$$\widehat{S}_d(\varphi_d, \lambda_d) = \sum_{\mathbb{P} \in \mathcal{X}_d^{\mathbb{P}}} \left[\mathcal{L}_d(j^1\varphi_d(\mathbb{P})) + \sum_{\ell=1}^4 \lambda_d^\ell(\mathbb{P})(J_\ell(\mathbb{P}) - 1) \right], \quad (52)$$

which imposes the equality constraint $J_\ell(\mathbb{P}) = 1$ for the discrete Jacobian, for all parallelepiped \mathbb{P} and all $\ell = 1, 2, 3, 4$. The critical point condition associated to (52) reads

$$\nabla_{\varphi_d} \widehat{S}_d(\bar{\varphi}_d, \bar{\lambda}_d) = 0 \quad \text{and} \quad J_d(\mathbb{P}) - 1 = 0 \quad \text{on all } \mathbb{P} \in \mathcal{X}_d^{\mathbb{P}}. \quad (53)$$

It is well-known, [33, p.187], that if $\bar{\varphi}_d$ is a local optimal solution of the function $S_d(\varphi_d)$ in (32) restricted to the discrete incompressibility equality constraint $\mathcal{C}_d = \{\varphi_d \mid J_\ell(\mathbb{D}) = 1, \forall \mathbb{D} \in \mathcal{X}_d^{\mathbb{D}}\}$, then there must be a Lagrangian multiplier $\bar{\lambda}_d$ such that (53) holds. However, solving the equations in (53) may not be practical, because inequality constraints also naturally appear, as we will see in the following examples. Let us thus consider a constraint set \mathcal{C}_d associated to the equality constraint $J_\ell = 1$ and to inequality constraints $g_i \leq 0$ for $i = 1, \dots, m$, i.e.,

$$\mathcal{C}_d = \{\varphi_d \mid J_\ell(\mathbb{D}) = 1 \text{ and } g_i(\mathbb{D}) \leq 0 \text{ for } i = 1, \dots, m\}. \quad (54)$$

Under appropriate conditions, see [34], generalizations of the Lagrangian multiplier rule allow to find the critical points of the action S_d defined in (32) under constraints of the form (54), see [9] for an application to variational integrators. In particular, we have the following necessary condition for $\bar{\varphi}_d \in \mathcal{C}_d$ to be locally optimal: $-\nabla S_d(\bar{\varphi}_d) \in N_{\mathcal{C}_d}(\bar{\varphi}_d)$, where $N_{\mathcal{C}_d}(\bar{\varphi}_d)$ is the normal cone to \mathcal{C}_d at $\bar{\varphi}_d$, which can be viewed as a special case of the calculus of subgradients, i.e., $N_{\mathcal{C}_d}(\bar{\varphi}_d) = \partial I_{\mathcal{C}_d}(\bar{\varphi}_d)$, where $I_{\mathcal{C}_d}$ is the indicator function of \mathcal{C}_d .

When \mathcal{C}_d and S_d are convex, the locally optimal condition is sufficient for $\bar{\varphi}_d$ to be globally optimal. If the ambient space is $\mathcal{M} = \mathbb{R}^n$, this relation reduces to

$$\nabla S_d(\bar{\varphi}_d) + \bar{\lambda}_0^\ell \nabla J_\ell(\bar{\varphi}_d) + \bar{\lambda}_1 \nabla g_1(\bar{\varphi}_d) + \dots + \bar{\lambda}_m \nabla g_m(\bar{\varphi}_d) = 0, \quad (55)$$

for $\bar{\lambda}_0^\ell \in \mathbb{R}$ and where $\bar{\lambda}_i \geq 0$, for $i = 1, \dots, m$, is non-vanishing only when $g_i(\bar{\varphi}_d) = 0$. When S_d is not convex it is difficult, on a practical viewpoint, to find the global optimal among the set of local optimals, see e.g., [9].

Also, given the examples that we will study, where \mathcal{C}_d is convex, instead of solving our problem with the Lagrangian multiplier approach we will introduce quadratic penalty functions $r\alpha(\varphi_d)$ associated with (54), with penalty parameter r , which may be considered as an approximation of the indicator function $I_{\mathcal{C}_d}$, see [28, p.280]. Moreover, if we suppose that for each r there exists a solution $\varphi_r \in \mathcal{M}$ to the problem to minimize $S_d(\varphi_d) + r\alpha(\varphi_d)$ with $\varphi_d \in \mathcal{M}$, and that the sequence $\{\varphi_r\}$ is contained in a compact subset of \mathcal{M} , we know (see [2, p.477]) that the limit $\bar{\varphi}_d$ of any convergent subsequence of $\{\varphi_r\}$ when $r \rightarrow \infty$ is an optimal solution to the original problem. If \mathcal{C}_d is nonconvex, a large enough penalty parameter r must be used to get sufficiently close to an optimal solution. In this case computational difficulties could appear to solve the penalty problem and an augmented Lagrangian penalty function can be considered, which enjoys several advantageous properties, see, e.g., [33, 34, 2].

Penalty method. Given the discrete action S_d defined in (32), the Hamilton principle subject to constraints is approximated by a penalty scheme where one seeks the critical points of the action

$$\tilde{S}_d(\varphi_d) = S_d(\varphi_d) - \sum_{\mathbb{D} \in \mathcal{X}_d^{\mathbb{D}}} \text{vol}(\mathbb{D}) (\Phi_{d0}(j^1 \varphi_d(\mathbb{D})) + \Phi_{d1}(j^1 \varphi_d(\mathbb{D})) + \dots + \Phi_{dm}(j^1 \varphi_d(\mathbb{D}))), \quad (56)$$

with quadratic penalty term associated to the incompressibility (equality) constraint

$$\Phi_{d0}(j^1\varphi_d(\mathbb{D})) := \frac{1}{4} \sum_{\ell=1}^4 \frac{r}{2} (J_\ell(\mathbb{D}) - 1)^2, \quad (57)$$

where r is the penalty parameter, and with quadratic penalty terms $\Phi_{di}(j^1\varphi_d(\mathbb{D}))$, $i = 2, \dots, m$, associated to inequality constraints.

3.2.1 Implicit version

To test the convergence of our multisymplectic integrator, we will use an implicit integrator obtained from the Lagrangian (27) discretized through the mid-point rule, that is, the discrete internal energy $W_d(\rho_0, j^1\varphi_d(\mathbb{D}_{a,b}^j))$ is evaluated at time $(t^j + t^{j+1})/2$. In this case the four vectors (22) at each node $(j, a, b) \in \mathcal{U}_d$ are now defined by

$$\begin{aligned} \mathbf{F}_{1;a,b}^{j+1/2} &= \frac{(\varphi_{a+1,b}^j + \varphi_{a+1,b}^{j+1}) - (\varphi_{a,b}^j + \varphi_{a,b}^{j+1})}{2\Delta s_1}, & \mathbf{F}_{2;a,b}^{j+1/2} &= \frac{(\varphi_{a,b+1}^j + \varphi_{a,b+1}^{j+1}) - (\varphi_{a,b}^j + \varphi_{a,b}^{j+1})}{2\Delta s_2} \\ \mathbf{F}_{3;a,b}^{j+1/2} &= \frac{(\varphi_{a-1,b}^j + \varphi_{a-1,b}^{j+1}) - (\varphi_{a,b}^j + \varphi_{a,b}^{j+1})}{2\Delta s_1}, & \mathbf{F}_{4;a,b}^{j+1/2} &= \frac{(\varphi_{a,b-1}^j + \varphi_{a,b-1}^{j+1}) - (\varphi_{a,b}^j + \varphi_{a,b}^{j+1})}{2\Delta s_2}. \end{aligned} \quad (58)$$

The variation $\delta S_d(\varphi_d)$ of the action sum is found as

$$\begin{aligned} & \sum_{j=0}^{N-1} \sum_{a=0}^{A-1} \sum_{b=0}^{B-1} \left[\left(\frac{M}{4} v_{a,b}^j + \mathbb{A}_{a,b}^j \right) \cdot \delta\varphi_{a,b}^{j+1} + \left(\frac{M}{4} v_{a+1,b}^j + \mathbb{B}_{a,b}^j \right) \cdot \delta\varphi_{a+1,b}^{j+1} \right. \\ & \quad + \left(\frac{M}{4} v_{a,b+1}^j + \mathbb{C}_{a,b}^j \right) \cdot \delta\varphi_{a,b+1}^{j+1} + \left(\frac{M}{4} v_{a+1,b+1}^j + \mathbb{D}_{a,b}^j \right) \cdot \delta\varphi_{a+1,b+1}^{j+1} \\ & \quad + \left(-\frac{M}{4} v_{a,b}^j + \mathbb{A}_{a,b}^j \right) \cdot \delta\varphi_{a,b}^j + \left(-\frac{M}{4} v_{a+1,b}^j + \mathbb{B}_{a,b}^j \right) \cdot \delta\varphi_{a+1,b}^j \\ & \quad \left. + \left(-\frac{M}{4} v_{a,b+1}^j + \mathbb{C}_{a,b}^j \right) \cdot \delta\varphi_{a,b+1}^j + \left(-\frac{M}{4} v_{a+1,b+1}^j + \mathbb{D}_{a,b}^j \right) \cdot \delta\varphi_{a+1,b+1}^j \right], \end{aligned}$$

with coefficients $\mathbb{A}_{a,b}^j$, $\mathbb{B}_{a,b}^j$, $\mathbb{C}_{a,b}^j$, $\mathbb{D}_{a,b}^j$ given in Appendix A.1 for an arbitrary internal energy function W . It yields the implicit discrete Euler-Lagrange equations

$$Mv_{a,b}^{j-1} - Mv_{a,b}^j + \mathbb{A}_{a,b}^j + \mathbb{A}_{a,b}^{j-1} + \mathbb{B}_{a-1,b}^j + \mathbb{B}_{a-1,b}^{j-1} + \mathbb{C}_{a,b-1}^j + \mathbb{C}_{a,b-1}^{j-1} + \mathbb{D}_{a-1,b-1}^j + \mathbb{D}_{a-1,b-1}^{j-1} = 0, \quad (59)$$

with the spatial boundary conditions

$$\begin{aligned} & \frac{M}{2} v_{0,b}^{j-1} - \frac{M}{2} v_{0,b}^j + \mathbb{A}_{0,b}^j + \mathbb{A}_{0,b}^{j-1} + \mathbb{C}_{0,b-1}^j + \mathbb{C}_{0,b-1}^{j-1} = 0, \\ & \frac{M}{2} v_{a,0}^{j-1} - \frac{M}{2} v_{a,0}^j + \mathbb{A}_{a,0}^j + \mathbb{A}_{a,0}^{j-1} + \mathbb{B}_{a-1,0}^j + \mathbb{B}_{a-1,0}^{j-1} = 0, \\ & \frac{M}{2} v_{A,b}^{j-1} - \frac{M}{2} v_{A,b}^j + \mathbb{B}_{A-1,b}^j + \mathbb{B}_{A-1,b}^{j-1} + \mathbb{D}_{A-1,b-1}^j + \mathbb{D}_{A-1,b-1}^{j-1} = 0, \\ & \frac{M}{2} v_{a,B}^{j-1} - \frac{M}{2} v_{a,B}^j + \mathbb{C}_{a,B-1}^j + \mathbb{C}_{a,B-1}^{j-1} + \mathbb{D}_{a-1,B-1}^j + \mathbb{D}_{a-1,B-1}^{j-1} = 0, \\ & \frac{M}{4} v_{0,0}^{j-1} - \frac{M}{4} v_{0,0}^j + \mathbb{A}_{0,0}^j + \mathbb{A}_{0,0}^{j-1} = 0, \quad \frac{M}{4} v_{A,0}^{j-1} - \frac{M}{4} v_{A,0}^j + \mathbb{B}_{A-1,0}^j + \mathbb{B}_{A-1,0}^{j-1} = 0, \\ & \frac{M}{4} v_{0,B}^{j-1} - \frac{M}{4} v_{0,B}^j + \mathbb{C}_{0,B-1}^j + \mathbb{C}_{0,B-1}^{j-1} = 0, \quad \frac{M}{4} v_{A,B}^{j-1} - \frac{M}{4} v_{A,B}^j + \mathbb{D}_{A-1,B-1}^j + \mathbb{D}_{A-1,B-1}^{j-1} = 0. \end{aligned} \quad (60)$$

The corresponding temporal boundary conditions can be computed similarly.

3.3 Numerical simulation

We evaluate the properties of the proposed multisymplectic integrator for barotropic and incompressible ideal fluid models with the case of a free boundary fluid and with the case of a fluid flowing on a surface and impacting an obstacle. In the two cases we present an explicit integrator, while we consider an implicit integrator (mid-point rule) for the convergence tests.

3.3.1 Example 1: fluid motion in vacuum with free boundaries

Consider a barotropic fluid with properties $\rho_0 = 997 \text{ kg/m}^3$, $\gamma = 6$, $A = \tilde{A}\rho_0^{-\gamma}$ with $\tilde{A} = 3.041 \times 10^4 \text{ Pa}$, and $B = 3.0397 \times 10^4 \text{ Pa}$. The size of the discrete reference configuration at time t^0 is $1\text{m} \times 1\text{m}$, with space-steps $\Delta s_1 = \Delta s_2 = 0.0714\text{m}$. We consider both the compressible barotropic fluid ($r = 0$) and the incompressible case with penalty parameters $r = 10^6$ and $r = 10^7$. The time-steps are $\Delta t = 10^{-3}$ when $r \in \{0, 10^6\}$, and $\Delta t = 5 \times 10^{-4}$ when $r = 10^7$. Initial perturbations (tiny compression) are applied at time t^1 on nodes $(4, 0)$ and $(5, 1)$. Note that in the incompressible case, using the penalty approach allows to treat this slight compression as initial condition.

Regarding the incompressible models, in the continuous setting the internal energy W plays no role since its effect is absorbed into the gradient of the pressure. In the discrete case, when using the penalty method for incompressible fluids it is advantageous to include the internal energy of the isentropic perfect fluid, as the case $W = 0$ needs to deal with a much higher penalty term.

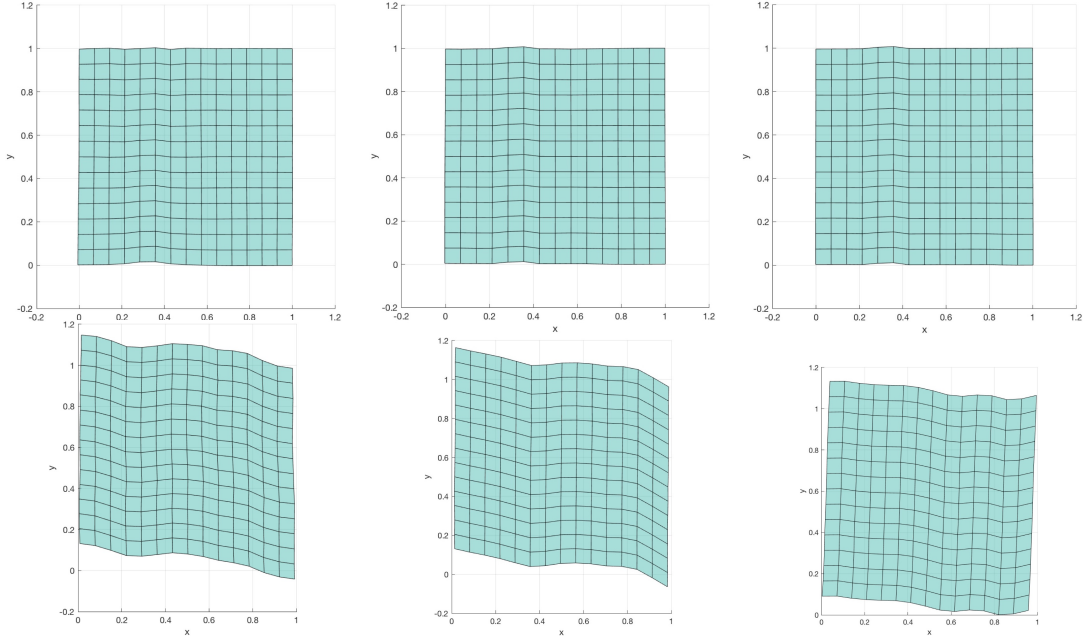


Figure 5: *Left to right*: barotropic and incompressible ideal fluid models ($r = 10^6$ and $r = 10^7$). *Top to bottom*: after 0.1s and 6s.

We observe that the compressible model exhibits enhanced deformation. The different behavior of the compressible and incompressible model will be even more noticeable in the following test, see Fig. 8 with respect to Fig. 7.

The discrete Lagrangian is invariant under rotation and translation, hence from the discrete Noether theorem the angular and linear momentum map (51) are preserved. Energy and momentum preservation is illustrated in Fig. 6.

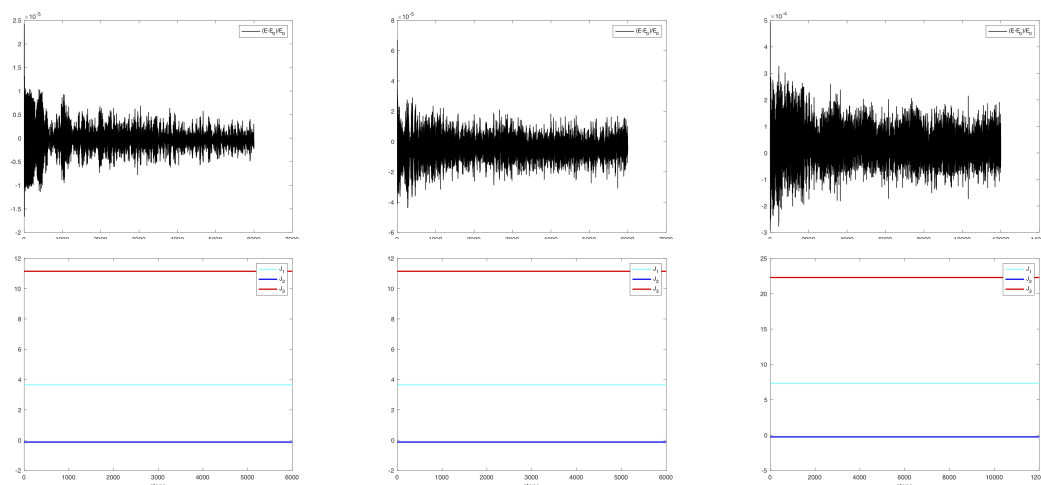


Figure 6: *Left to right*: barotropic and incompressible ideal fluid models ($r = 10^6$ and $r = 10^7$). *Top to bottom*: Relative energy and momentum map evolution during 6s.

3.3.2 Example 2: impact against an obstacle of a fluid flowing on a surface

Inequality constraint. Let us consider a fluid subject to gravity and flowing without friction on a surface until it comes into contact with an obstacle. The gravitational potential is described by (31) with $\mathbf{g} = g\mathbf{E}_2$. We consider both a barotropic fluid and an incompressible ideal fluid.

We impose the following constraints on the configuration:

- The fluid is bounded below by a rigid surface, defined by the inequality constraint $\Psi_1(\varphi_{a,b}^j) \leq 0$ verified for all $\varphi_{a,b}^j$.
- There is a second inequality constraint $\Psi_2(\varphi_{a,b}^j) \leq 0$, verified for all $\varphi_{a,b}^j$, which forces the fluid to stay outside of the obstacle.

For barotropic fluid and incompressible ideal fluid the problems to solve are respectively described as follows

- (\mathcal{P}_1) Find the critical points of the action S_d defined in (32) subject to the inequality constraints $\Psi_\alpha(\varphi_{a,b}^j) \leq 0$, $\alpha = 1, 2$, for all nodes.

- (\mathcal{P}_2) Find the critical points of the action S_d defined in (32) subject to the equality constraint $J_\ell(\mathbb{D}) = 1$, see (52), and the inequality constraints $\Psi_\alpha(\varphi_{a,b}^j) \leq 0$, $\alpha = 1, 2$, for all nodes.

We solve the previous problems via the penalty method. For problem \mathcal{P}_1 , we must find the critical points of the action

$$\tilde{S}_d(\varphi_d) = S_d(\varphi_d) - \sum_{j=0}^{N-1} \sum_{a=0}^{A-1} \sum_{b=0}^{B-1} \Delta t \Delta s_1 \Delta s_2 \left(\Phi_{d1}(\varphi_{a,b}^j) + \Phi_{d2}(\varphi_{a,b}^j) \right), \quad (61)$$

$$\Phi_{d\alpha}(\varphi_{a,b}^j) = \frac{1}{2} K_\alpha |\Psi_\alpha(\varphi_{a,b}^j)|^2 \quad \text{with} \quad \begin{cases} K_\alpha \in]0, \infty[& \text{if } \Psi_\alpha(\varphi_{a,b}^j) \geq 0 \\ K_\alpha = 0 & \text{if } \Psi_\alpha(\varphi_{a,b}^j) < 0 \end{cases}. \quad (62)$$

For problem \mathcal{P}_2 we add the penalty function (57), associated to the equality constraint $J^\ell(\mathbb{D}) = 1$, into the discrete action (61).

Test. Consider a barotropic fluid model with properties $\rho_0 = 997 \text{ kg/m}^3$, $\gamma = 6$, $A = \tilde{A} \rho_0^{-\gamma}$ with $\tilde{A} = 3.041 \times 10^4 \text{ Pa}$, and $B = 3.0397 \times 10^4 \text{ Pa}$. The size of the discrete reference configuration at time t^0 is $2 \text{ m} \times 0.4 \text{ m}$, with time-step $\Delta t = 10^{-4}$ and space-steps $\Delta s_1 = 0.0625 \text{ m}$, $\Delta s_2 = 0.033 \text{ m}$. The values of the impenetrability penalty parameters are chosen as $K_1 = 4.8 \times 10^{10}$, $K_2 = 4.8 \times 10^6$. For the incompressible case we consider the penalty parameter $r = 5 \times 10^8$.

The initial motion of the fluid is only due to the gravity. There are no other perturbations so that there is no expansion or compression imposed in the initial conditions. The evolution in the barotropic and incompressible cases are illustrated in Fig. 7 and Fig. 8, with the incompressibility conditions imposed by the penalty term.

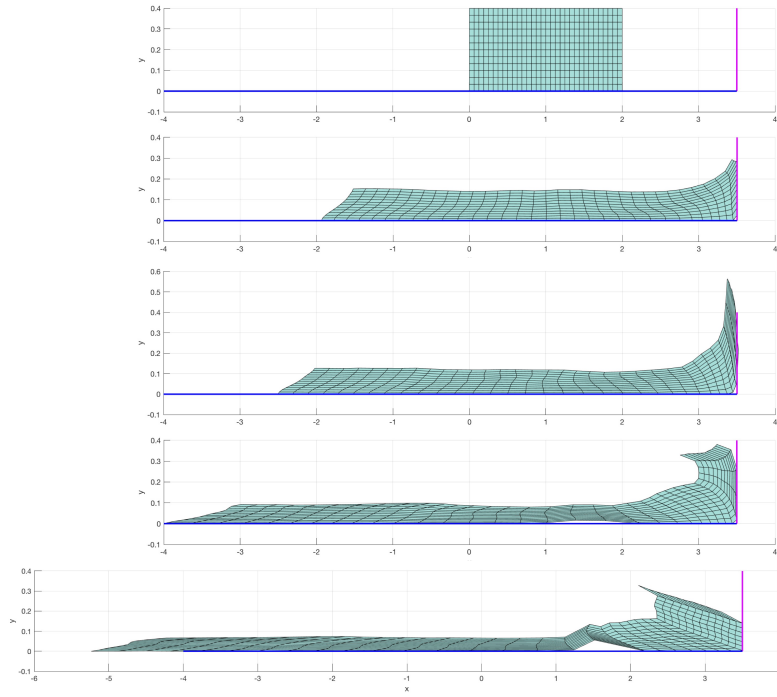


Figure 7: Barotropic fluid with contact. *Top to bottom*: after 0.01s, 1s, 1.2s, 1.6s, 2s.

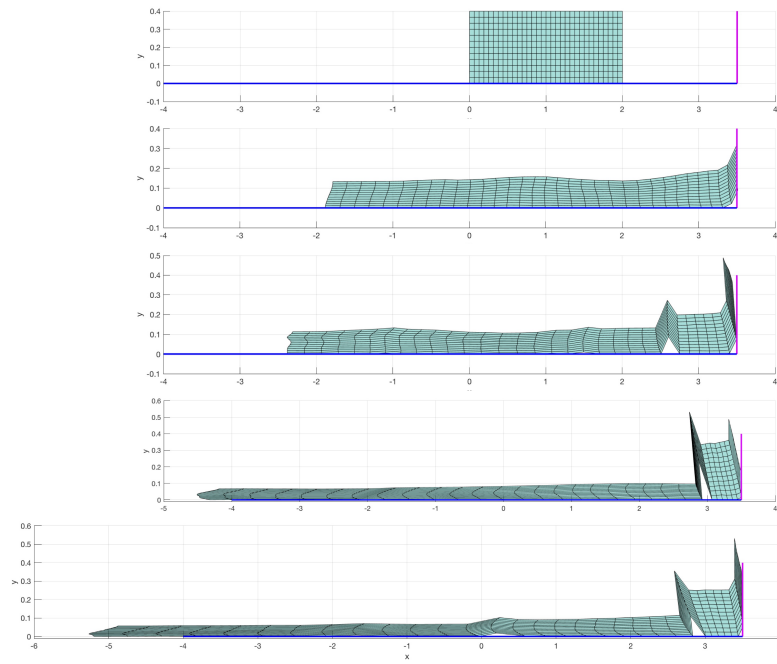


Figure 8: Incompressible ideal fluid with contact. *Top to bottom*: after 0.01s, 1s, 1.2s, 1.8s, 2s.

The momentum map evolution is given in Fig. 9, where we note that only the component of the momentum map associated with vertical translation is preserved before the impact because of the presence of the gravity term. The energy perturbation increases after the contact, while complex phenomena similar to those encountered in breaking waves appear, like plunging waves, giving rise to a turbulent motion.

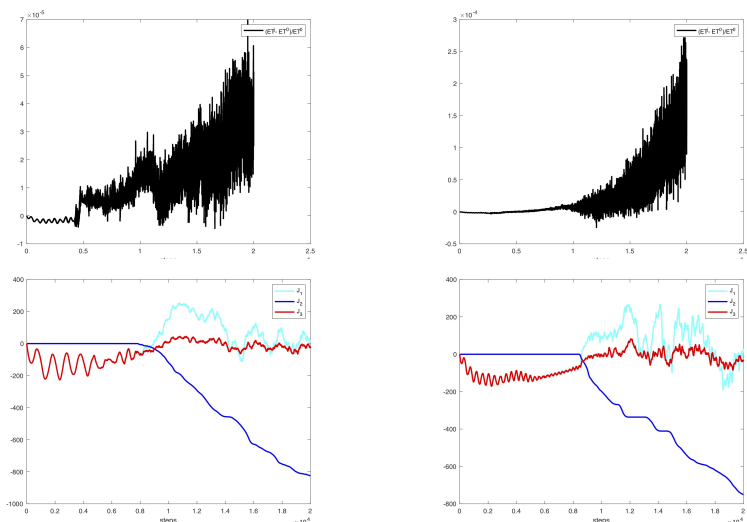


Figure 9: *Left to right* Barotropic fluid and incompressible ideal fluid with contact. *Top to bottom*: Relative energy and momentum map evolution during 2s.

3.3.3 Convergence tests

Consider a barotropic fluid model with properties $\rho_0 = 997 \text{ kg/m}^2$, $\gamma = 6$, $A = \tilde{A}\rho_0^{-\gamma}$ with $\tilde{A} = 3.041 \times 10^4 \text{ Pa}$, and $B = 3.0397 \times 10^4 \text{ Pa}$. The size of the discrete reference configuration at time t^0 is $0.4 \text{ m} \times 0.4 \text{ m}$. We consider the *implicit* integrator to study the convergence with respect to Δt and $\Delta s_1 = \Delta s_2$.

Barotropic fluid motion in vacuum with free boundaries. Given a fixed mesh, with values $\Delta s_1 = \Delta s_2 = 0.057 \text{ m}$, we impose an initial speed $V_{a,0}^0 = (0, 0.163 \times a)^T$ on the boundary $b = 0$ for all $a \in \{0, \dots, A\}$, and vary the time-steps as $\Delta t \in \{5 \times 10^{-3}, 2.5 \times 10^{-3}, 1.25 \times 10^{-3}, 6.25 \times 10^{-4}\}$. We compute the L^2 -errors in the position φ_d at time $t^N = 0.25 \text{ s}$, by comparing φ_d with an “exact solution” obtained with the time-step $\Delta t_{\text{ref}} = 3.125 \times 10^{-4} \text{ s}$. That is, for each value of Δt we calculate

$$\|\varphi_d - \varphi_{\text{ref}}\|_{L^2} = \left(\sum_a \sum_b \|\varphi_{a,b}^N - \varphi_{\text{ref};a,b}^N\|^2 \right)^{1/2}. \quad (63)$$

This yields the following convergence with respect to Δt

Δt	5×10^{-3}	2.5×10^{-3}	1.25×10^{-3}	6.25×10^{-4}
$\ \varphi_d - \varphi_{\text{ref}}\ _{L^2}$	1.5×10^{-2}	7×10^{-3}	3.6×10^{-3}	1×10^{-3}
rate		1.106	0.964	1.815

Given a fixed time-step $\Delta t = 2 \times 10^{-3}$ we impose an initial speed² $V_{a,0}^0 = (0, 0.163 \times a)^T$, on the boundary $b = 0$ for all $a \in \{0, \dots, A\}$, and vary the space-steps as $\Delta s_1 = \Delta s_2 \in \{0.4, 0.2, 0.1, 0.05\}$. The “exact solution” is chosen with $\Delta s_{1;\text{ref}} = \Delta s_{2;\text{ref}} = 0.025\text{m}$. We compute the L^2 -errors in the position φ_d at time $t^N = 0.1\text{s}$. We get the following convergence with respect to $\Delta s_1 = \Delta s_2$

$\Delta s_1 = \Delta s_2$	0.4	0.2	0.1	0.05
$\ \varphi_d - \varphi_{\text{ref}}\ _{L^2}$	3×10^{-2}	2.16×10^{-2}	1.53×10^{-2}	7.1×10^{-3}
rate		0.475	0.493	1.12

Impact against an obstacle of a fluid flowing on a surface. The values of the impenetrability penalty parameters are $K_1 = K_2 = 3 \times 10^7$. Given a fixed mesh, with values $\Delta s_1 = \Delta s_2 = 0.057\text{m}$, we repeat the experiment, described in Fig. 10, with varying values of $\Delta t \in \{5 \times 10^{-3}, 2.5 \times 10^{-3}, 1.25 \times 10^{-3}, 6.25 \times 10^{-4}\}$. Then, we compute the L^2 -errors in the position φ_d at time $t^N = 0.25\text{s}$, by comparing φ_d with an “exact solution” obtained with the time-step $\Delta t_{\text{ref}} = 3.125 \times 10^{-4}$. We get the following convergence with respect to Δt

Δt	5×10^{-3}	2.5×10^{-3}	1.25×10^{-3}	6.25×10^{-4}
$\ \varphi_d - \varphi_{\text{ref}}\ _{L^2}$	7.5×10^{-2}	3.5×10^{-2}	1.5×10^{-2}	5×10^{-3}
rate		1.101	1.226	1.586

Similarly, given a fixed time-step $\Delta t = 2 \times 10^{-3}$ we repeat the same experiment with varying values of $\Delta s_1 = \Delta s_2 \in \{0.4, 0.2, 0.1, 0.05\}$. The “exact solution” is chosen with $\Delta s_{1;\text{ref}} = \Delta s_{2;\text{ref}} = 0.025\text{m}$. We compute the L^2 -errors in the position φ_d at time $t^N = 0.1\text{s}$. Therefore we get the following convergence with respect to $\Delta s_1 = \Delta s_2$

$\Delta s_1 = \Delta s_2$	0.4	0.2	0.1	0.05
$\ \varphi_d - \varphi_{\text{ref}}\ _{L^2}$	6.38×10^{-2}	3.84×10^{-2}	1.75×10^{-2}	6.8×10^{-3}
rate		0.733	1.132	1.366

An illustration of the test used for the numerical convergence is given in Fig. 10.

²Note that, we need to take care of the initial sum of momentum $\sum_a m_a V_{a,0}^0$ which must be of the same value regardless of the number of nodes in the mesh.

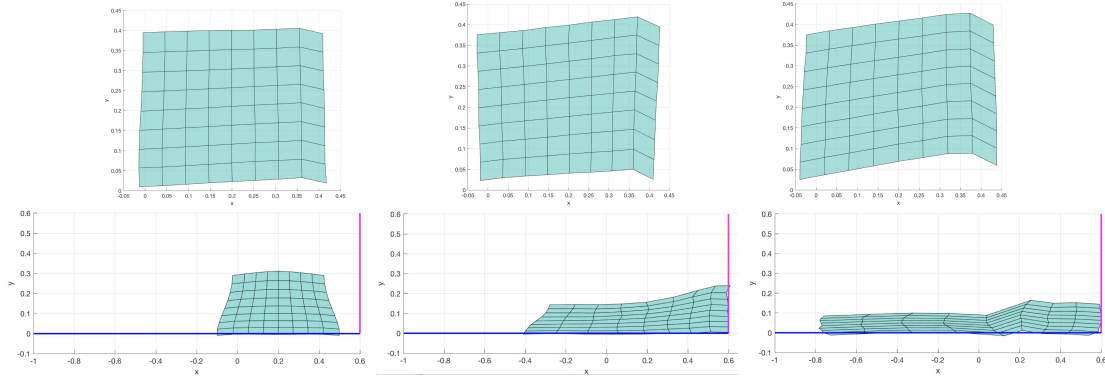


Figure 10: Barotropic fluid. *From top to bottom*: motion in vacuum with free boundaries ($\Delta s_1 = \Delta s_2 = 0.05$, $\Delta t = 2 \times 10^{-3}$), and impact against an obstacle of a fluid flowing on a surface ($\Delta s_1 = \Delta s_2 = 0.05$, $\Delta t = 2 \times 10^{-3}$). *From left to right*: after 0.15s, 0.3s, and 0.5s.

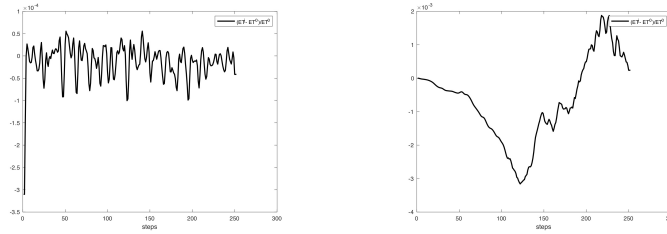


Figure 11: Relative error in the energy $(ET^j - ET^0)/ET^0$, with ET^j the total energy at time t^j . *From left to right*: motion in vacuum with free boundaries ($\Delta s_1 = \Delta s_2 = 0.05$, $\Delta t = 2 \times 10^{-3}$), and impact against an obstacle of a fluid flowing on a surface ($\Delta s_1 = \Delta s_2 = 0.05$, $\Delta t = 2 \times 10^{-3}$).

4 3D discrete barotropic and incompressible fluid models

In this section we indicate how the developments made in §3 extend to the 3D case. The general discrete multisymplectic framework (discrete configuration bundle, discrete first jet, discrete multisymplectic form, etc...) have been already explained in a general setting in §3. We assume that \mathcal{B} is a parallelepiped in \mathbb{R}^3 and take $\mathcal{M} = \mathbb{R}^3$.

4.1 Multisymplectic discretizations

4.1.1 Discrete configuration bundle

The discrete parameter space \mathcal{U}_d is now decomposed in a set of elements $\mathcal{Q}_{a,b,c}^j$ defined by 16 pairs of indices, see Fig. 12 for the eight pairs of indices in $\mathcal{Q}_{a,b,c}^j$ at time t^j .

As in (21), we consider discrete base-space configurations of the form

$$\phi_{\mathcal{X}_d} : \mathcal{U}_d \ni (j, a, b, c) \mapsto s_{a,b,c}^j = (t^j, z_a^j, z_b^j, z_c^j) \in \mathcal{X}_d \subset \mathbb{R} \times \mathcal{B}. \quad (64)$$

The discrete field φ_d evaluated at $s_{a,b,c}^j$ is denoted $\varphi_{a,b,c}^j := \varphi_d(s_{a,b,c}^j) \in \mathbb{R}^3$.

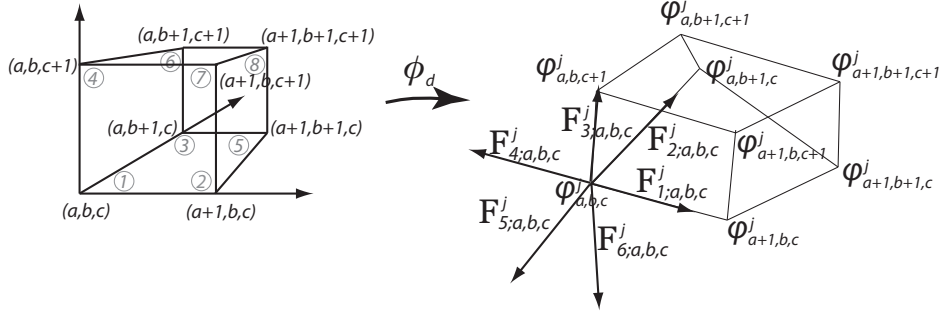


Figure 12: Discrete field $\phi_d = \varphi_d \circ \phi_{\mathcal{X}_d}$ evaluated on $\mathbb{E}_{a,b,c}^j$ at time t^j .

4.1.2 Discrete Jacobian

Given a discrete base space configuration $\phi_{\mathcal{X}_d}$ of the form (64) and a discrete field φ_d , we define the following six vectors $\mathbf{F}_{\ell;a,b,c}^j \in \mathbb{R}^3$, $\ell = 1, \dots, 6$ at each node $(j, a, b, c) \in \mathcal{U}_d$, see Fig. 12 on the right:

$$\begin{aligned} \mathbf{F}_{1;a,b,c}^j &= \frac{\varphi_{a+1,b,c}^j - \varphi_{a,b,c}^j}{|s_{a+1,b,c} - s_{a,b,c}|}, & \mathbf{F}_{2;a,b,c}^j &= \frac{\varphi_{a,b+1,c}^j - \varphi_{a,b,c}^j}{|s_{a,b+1,c} - s_{a,b,c}|}, \\ \mathbf{F}_{3;a,b,c}^j &= \frac{\varphi_{a,b,c+1}^j - \varphi_{a,b,c}^j}{|s_{a,b,c+1} - s_{a,b,c}|}, & \mathbf{F}_{4;a,b,c}^j &= \frac{\varphi_{a-1,b,c}^j - \varphi_{a,b,c}^j}{|s_{a,b,c} - s_{a-1,b,c}|} = -\mathbf{F}_{1;a-1,b,c}^j \\ \mathbf{F}_{5;a,b,c}^j &= \frac{\varphi_{a,b-1,c}^j - \varphi_{a,b,c}^j}{|s_{a,b,c} - s_{a,b-1,c}|} = -\mathbf{F}_{2;a,b-1,c}^j, & \mathbf{F}_{6;a,b,c}^j &= \frac{\varphi_{a,b,c-1}^j - \varphi_{a,b,c}^j}{|s_{a,b,c} - s_{a,b,c-1}|} = -\mathbf{F}_{3;a,b,c-1}^j. \end{aligned}$$

Based on these definitions, the discrete gradient is constructed as follows.

Definition 4.1 *The discrete gradient deformations of a discrete field φ_d at the element $\mathbb{E}_{a,b,c}^j$ are the 3×3 matrices $\mathbf{F}^\ell(\mathbb{E}_{a,b,c}^j)$, $\ell = 1, \dots, 8$, defined at the eight nodes at time t^j of $\mathbb{E}_{a,b,c}^j$ as follows:*

$$\begin{aligned} \mathbf{F}_1(\mathbb{E}_{a,b,c}^j) &= \begin{bmatrix} \mathbf{F}_{1;a,b,c}^j & \mathbf{F}_{2;a,b,c}^j & \mathbf{F}_{3;a,b,c}^j \end{bmatrix}, \\ \mathbf{F}_2(\mathbb{E}_{a,b,c}^j) &= \begin{bmatrix} \mathbf{F}_{2;a+1,b,c}^j & \mathbf{F}_{4;a+1,b,c}^j & \mathbf{F}_{3;a+1,b,c}^j \end{bmatrix}, \\ \mathbf{F}_3(\mathbb{E}_{a,b,c}^j) &= \begin{bmatrix} \mathbf{F}_{5;a,b+1,c}^j & \mathbf{F}_{1;a,b+1,c}^j & \mathbf{F}_{3;a,b+1,c}^j \end{bmatrix}, \\ \mathbf{F}_4(\mathbb{E}_{a,b,c}^j) &= \begin{bmatrix} \mathbf{F}_{2;a,b,c+1}^j & \mathbf{F}_{1;a,b,c+1}^j & \mathbf{F}_{6;a,b,c+1}^j \end{bmatrix}, \\ \mathbf{F}_5(\mathbb{E}_{a,b,c}^j) &= \begin{bmatrix} \mathbf{F}_{4;a+1,b+1,c}^j & \mathbf{F}_{5;a+1,b+1,c}^j & \mathbf{F}_{3;a+1,b+1,c}^j \end{bmatrix}, \\ \mathbf{F}_6(\mathbb{E}_{a,b,c}^j) &= \begin{bmatrix} \mathbf{F}_{1;a,b+1,c+1}^j & \mathbf{F}_{5;a,b+1,c+1}^j & \mathbf{F}_{6;a,b+1,c+1}^j \end{bmatrix}, \\ \mathbf{F}_7(\mathbb{E}_{a,b,c}^j) &= \begin{bmatrix} \mathbf{F}_{4;a+1,b,c+1}^j & \mathbf{F}_{2;a+1,b,c+1}^j & \mathbf{F}_{6;a+1,b,c+1}^j \end{bmatrix}, \\ \mathbf{F}_8(\mathbb{E}_{a,b,c}^j) &= \begin{bmatrix} \mathbf{F}_{5;a+1,b+1,c+1}^j & \mathbf{F}_{4;a+1,b+1,c+1}^j & \mathbf{F}_{6;a+1,b,c+1}^j \end{bmatrix}. \end{aligned} \tag{65}$$

The ordering $\ell = 1$ to $\ell = 8$ is respectively associated to the nodes (j, a, b, c) , $(j, a+1, b, c)$, $(j, a, b+1, c)$, $(j, a, b, c+1)$, $(j, a+1, b+1, c)$, $(j, a, b+1, c+1)$, $(j, a+1, b, c+1)$, $(j, a+1, b+1, c+1)$, see Fig. 12 on the left.

Then we define the Jacobian in each node, as follows

Definition 4.2 The discrete Jacobians of a discrete field φ_d at the element $\mathbb{E}_{a,b,c}^j$ are the numbers $J_\ell(\mathbb{E}_{a,b}^j)$, $\ell = 1, \dots, 8$, defined at the eight nodes at time t^j of $\mathbb{E}_{a,b,c}^j$ as follows:

$$J_1(\mathbb{E}_{a,b,c}^j) = (\mathbf{F}_{1;a,b,c}^j \times \mathbf{F}_{2;a,b,c}^j) \cdot \mathbf{F}_{3;a,b,c}^j = \det(\mathbf{F}_1(\mathbb{E}_{a,b,c}^j)). \quad (66)$$

See in §A.3 for the others Jacobian on $\mathbb{E}_{a,b,c}^j$. We can now establish the link between the discrete Jacobian and the discrete gradient deformation.

In terms of the discrete field φ_d , the discrete Jacobians are

$$J_1(\mathbb{E}_{a,b,c}^j) = \frac{((\varphi_{a+1,b,c}^j - \varphi_{a,b,c}^j) \times (\varphi_{a,b+1,c}^j - \varphi_{a,b,c}^j)) \cdot (\varphi_{a,b,c+1}^j - \varphi_{a,b,c}^j)}{|s_{a+1,b,c} - s_{a,b,c}| |s_{a,b+1,c} - s_{a,b,c}| |s_{a,b,c+1} - s_{a,b,c}|}$$

$$J_2(\mathbb{E}_{a,b,c}^j) = \frac{((\varphi_{a+1,b+1,c}^j - \varphi_{a+1,b,c}^j) \times (\varphi_{a,b,c}^j - \varphi_{a+1,b,c}^j)) \cdot (\varphi_{a+1,b,c+1}^j - \varphi_{a+1,b,c}^j)}{|s_{a+1,b+1,c} - s_{a+1,b,c}| |s_{a,b,c} - s_{a+1,b,c}| |s_{a+1,b,c+1} - s_{a+1,b,c}|}$$

similarly for the other ones.

4.1.3 Discrete Lagrangian

The discrete Lagrangian for 3D barotropic fluid models has the same general form as (27), with the obvious 3D extension of formulas (28)–(31).

4.1.4 Discrete variations and discrete Euler-Lagrange equations

The discrete action functional takes the form

$$S_d(\varphi_d) = \sum_{j=0}^{N-1} \sum_{a=0}^{A-1} \sum_{b=0}^{B-1} \sum_{c=0}^{C-1} \mathcal{L}(j^1 \varphi_d(\mathbb{E}_{a,b,c}^j)) \quad (67)$$

and yield the discrete Euler-Lagrange equations

$$Mv_{a,b,c}^j + A_{a,b,c}^j + B_{a-1,b,c}^j + C_{a,b-1,c}^j + D_{a,b,c-1}^j + E_{a-1,b-1,c}^j + F_{a,b-1,c-1}^j + G_{a-1,b,c-1}^j + H_{a-1,b-1,c-1}^j = 0, \quad (68)$$

where we have used notations analogous to (33) and (34) for the partial derivative of \mathcal{L}_d . We refer to Appendix A.4 for the expressions of $A_{a,b,c}^j, \dots, H_{a,b,c}^j$. Boundary conditions are deduced the discrete Hamilton principle in a similar way as it was done in (36) and (37) for the 2D case.

4.1.5 Discrete multisymplectic form formula and discrete Noether theorem

Following the general definition (38), the discrete Cartan forms evaluated at the first jet extension $j^1\varphi_d(\mathbb{E}_{a,b,c}^j)$ of a discrete field φ_d are

$$\begin{aligned}
\Theta_{\mathcal{L}_d}^1 &= A_{a,b,c}^j d\varphi_{a,b,c}^j, & \Theta_{\mathcal{L}_d}^2 &= \frac{M}{8} v_{a,b,c}^j d\varphi_{a,b,c}^{j+1}, \\
\Theta_{\mathcal{L}_d}^3 &= B_{a,b,c}^j d\varphi_{a+1,b,c}^j, & \Theta_{\mathcal{L}_d}^4 &= \frac{M}{8} v_{a+1,b,c}^j d\varphi_{a+1,b,c}^{j+1}, \\
\Theta_{\mathcal{L}_d}^5 &= C_{a,b,c}^j d\varphi_{a,b+1,c}^j, & \Theta_{\mathcal{L}_d}^6 &= \frac{M}{8} v_{a,b+1,c}^{j+1} d\varphi_{a,b+1,c}^{j+1}, \\
\Theta_{\mathcal{L}_d}^7 &= D_{a,b,c}^j d\varphi_{a,b,c+1}^j, & \Theta_{\mathcal{L}_d}^8 &= \frac{M}{8} v_{a,b,c+1}^j d\varphi_{a,b,c+1}^{j+1}, \\
\Theta_{\mathcal{L}_d}^9 &= E_{a,b,c}^j d\varphi_{a+1,b+1,c}^j, & \Theta_{\mathcal{L}_d}^{10} &= \frac{M}{8} v_{a+1,b+1,c}^j d\varphi_{a+1,b+1,c}^{j+1}, \\
\Theta_{\mathcal{L}_d}^{11} &= F_{a,b,c}^j d\varphi_{a,b+1,c+1}^j, & \Theta_{\mathcal{L}_d}^{12} &= \frac{M}{8} v_{a,b+1,c+1}^j d\varphi_{a,b+1,c+1}^{j+1}, \\
\Theta_{\mathcal{L}_d}^{13} &= G_{a,b,c}^j d\varphi_{a+1,b,c+1}^j, & \Theta_{\mathcal{L}_d}^{14} &= \frac{M}{8} v_{a+1,b,c+1}^{j+1} d\varphi_{a+1,b,c+1}^{j+1}, \\
\Theta_{\mathcal{L}_d}^{15} &= H_{a,b,c}^j d\varphi_{a+1,b+1,c+1}^j, & \Theta_{\mathcal{L}_d}^{16} &= \frac{M}{8} v_{a+1,b+1,c+1}^j d\varphi_{a+1,b+1,c+1}^{j+1}.
\end{aligned} \tag{69}$$

With these forms, the discrete multisymplectic form formula and conservation laws in the presence of a symmetry group (discrete Noether theorem) can be derived in a similar way as it was done in 2D in §3.1.

4.1.6 Symmetries for barotropic fluids

Exactly as in §3.1.7, the discrete Lagrangian is $SE(3)$ invariant and hence the discrete covariant Noether theorem holds with the covariant discrete momentum maps $J_{\mathcal{L}_d}^{\mathbf{p}} : J^1\mathcal{Y}_d \rightarrow \mathfrak{se}(3)^*$, $\mathbf{p} = 1, \dots, 16$. From this, the discrete momentum map

$$\begin{aligned}
\mathbf{J}_d^j &= \mathbf{J}_d(\varphi^j, \varphi^{j+1}) = \sum_{a=0}^{A-1} \sum_{b=0}^{B-1} \sum_{c=0}^{C-1} (J_{\mathcal{L}_d}^2 + J_{\mathcal{L}_d}^4 + J_{\mathcal{L}_d}^6 + J_{\mathcal{L}_d}^8 + J_{\mathcal{L}_d}^{10} + J_{\mathcal{L}_d}^{12} + J_{\mathcal{L}_d}^{14} + J_{\mathcal{L}_d}^{16}) \\
&= - \sum_{a=0}^{A-1} \sum_{b=0}^{B-1} \sum_{c=0}^{C-1} (J_{\mathcal{L}_d}^1 + J_{\mathcal{L}_d}^3 + J_{\mathcal{L}_d}^5 + J_{\mathcal{L}_d}^7 + J_{\mathcal{L}_d}^9 + J_{\mathcal{L}_d}^{11} + J_{\mathcal{L}_d}^{13} + J_{\mathcal{L}_d}^{15}),
\end{aligned} \tag{70}$$

is preserved, as explained in §3.1.7. In 3D, the expression (51) extends as

$$\mathbf{J}_d^j = \begin{bmatrix} \sum_{a=0}^{A-1} \sum_{b=0}^{B-1} \sum_{a=0}^{C-1} \mathbf{J}_r(j^1\varphi_d(\mathbb{E}_{a,b}^j)) \\ \sum_{a=0}^{A-1} \sum_{b=0}^{B-1} \sum_{a=0}^{C-1} \mathbf{J}_l(j^1\varphi_d(\mathbb{E}_{a,b}^j)) \end{bmatrix}$$

with

$$\mathbf{J}_r(j^1\varphi_d(\mathbb{D}_{a,b,c}^j)) = \sum_{\alpha=a}^{a+1} \sum_{\beta=b}^{b+1} \sum_{\gamma=c}^{c+1} \varphi_{\alpha,\beta,\gamma}^j \times \left(\frac{M}{8} v_{\alpha,\beta,\gamma}^j \right) \in \mathbb{R}^3$$

$$\mathbf{J}_l(j^1\varphi_d(\mathbb{D}_{a,b,c}^j)) = \sum_{\alpha=a}^{a+1} \sum_{\beta=b}^{b+1} \sum_{\gamma=c}^{c+1} \frac{M}{8} v_{\alpha,\beta,\gamma}^j \in \mathbb{R}^3.$$

4.1.7 Incompressible ideal hydrodynamics

As done in 2D (see §3.2), associated to the equality constraint $J = 1$ we consider a penalty function

$$\Phi_{d0}(j^1\varphi_d(\mathbb{D})) := \frac{1}{8} \sum_{\ell=1}^8 \frac{r}{2} (J_\ell(\mathbb{D}) - 1)^2, \quad (71)$$

where r is the penalty parameter.

4.2 Numerical simulations

In this section we illustrate the performance of an explicit-in-time integrator in 3D³, as it was done in §3.3.

4.2.1 Example 3: barotropic fluid motion in vacuum with free boundaries

Consider a barotropic fluid with properties $\rho_0 = 997 \text{ kg/m}^3$, $\gamma = 6$, $A = \tilde{A}\rho_0^{-\gamma}$ with $\tilde{A} = 3.041 \times 10^4 \text{ Pa}$, and $B = 3.0397 \times 10^4 \text{ Pa}$. The size of the mesh at time t^0 is $2 \text{ m} \times 2 \text{ m} \times 2 \text{ m}$, with $\Delta s_1 = \Delta s_2 = \Delta s_3 = 0.333 \text{ m}$. We consider both the compressible barotropic fluid and the incompressible case with penalty parameter $r = 10^5$ and $r = 10^7$. The time step is $\Delta t = 10^{-3}$. There are no exterior forces.

Initial perturbations are applied at time t^1 on nodes $(1, 0, 1)$ and $(1, 0, 2)$, in a similar way with the test made in dimension 2, see Fig. 5.

³Note that with the multisymplectic variational integrators we can equally move in time and in space, see [8].

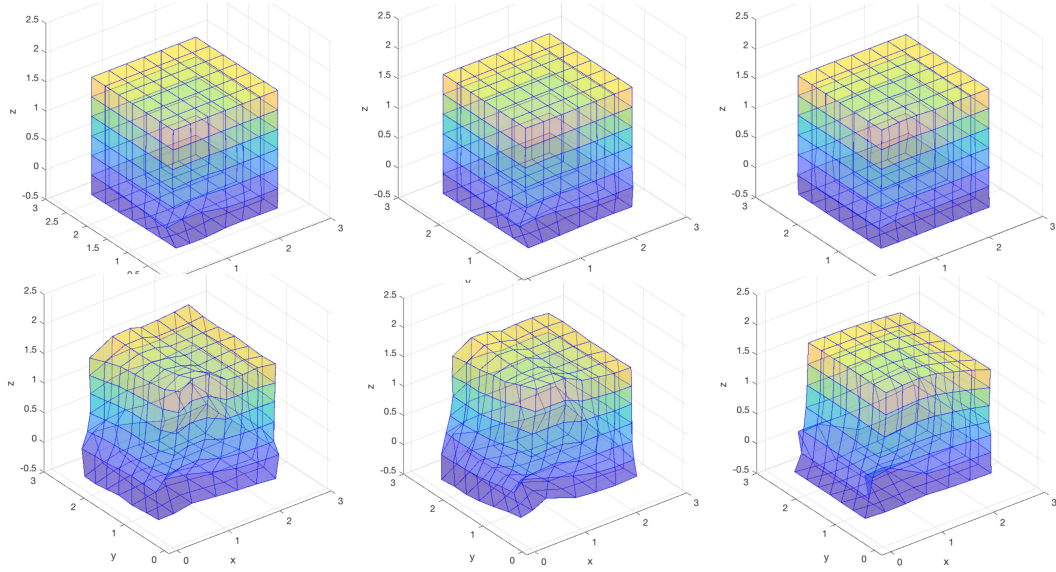


Figure 13: *Left to right*: Discrete barotropic and incompressible ideal fluid model ($r = 10^5$ and $r = 10^7$). *Top to bottom*: after 0.1s and 2s.

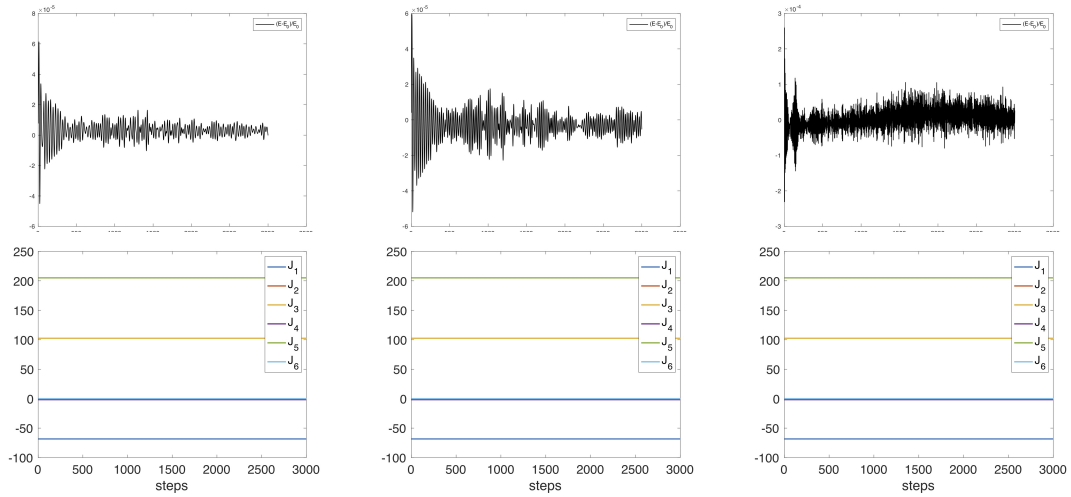


Figure 14: *Left to right*: barotropic and incompressible ideal fluid model ($r = 10^5$ and $r = 10^7$). *Top to bottom*: Relative energy and momentum map evolution during 3s.

The main interest of this test in vacuum with free boundaries is to exhibit the perfect preservation of the symmetries, see the figures above.

4.2.2 Example 4: Impact against an obstacle of a fluid flowing on a surface

As explain in §3.3.2, in this example the problems are to find the extremum of the action subject to an equality constraint associated to incompressibility and inequality constraints imposing the fluid to stay on a surface and outside of an obstacle.

Let (\mathcal{P}_1) , resp., (\mathcal{P}_2) denote the problem to solve for barotropic fluid, resp., incompressible ideal fluid. These two problems are already described in §3.3.2.

Consider a barotropic fluid with properties $\rho_0 = 997 \text{ kg/m}^3$, $\gamma = 7$, $A = \tilde{A}\rho_0^{-\gamma}$ with $\tilde{A} = 3.041 \times 10^4 \text{ Pa}$, and $B = 3.0397 \times 10^4 \text{ Pa}$. The size of the discrete reference configuration at time t^0 is $1.6 \text{ m} \times 1 \text{ m} \times 0.4 \text{ m}$, with time-step $\Delta t = 5 \times 10^{-5}$ and space-steps $\Delta s_1 = 0.1 \text{ m}$, $\Delta s_2 = 0.2 \text{ m}$, $\Delta s_3 = 0.1 \text{ m}$. The value of the impenetrability penalty coefficients are $K_1 = K_2 = 5 \times 10^9$. We consider both the compressible barotropic fluid and the incompressible case with penalty given by $r = 10^8$ and $r = 10^9$.

As in 2D, the initial motion of the fluid is only due to the gravity.

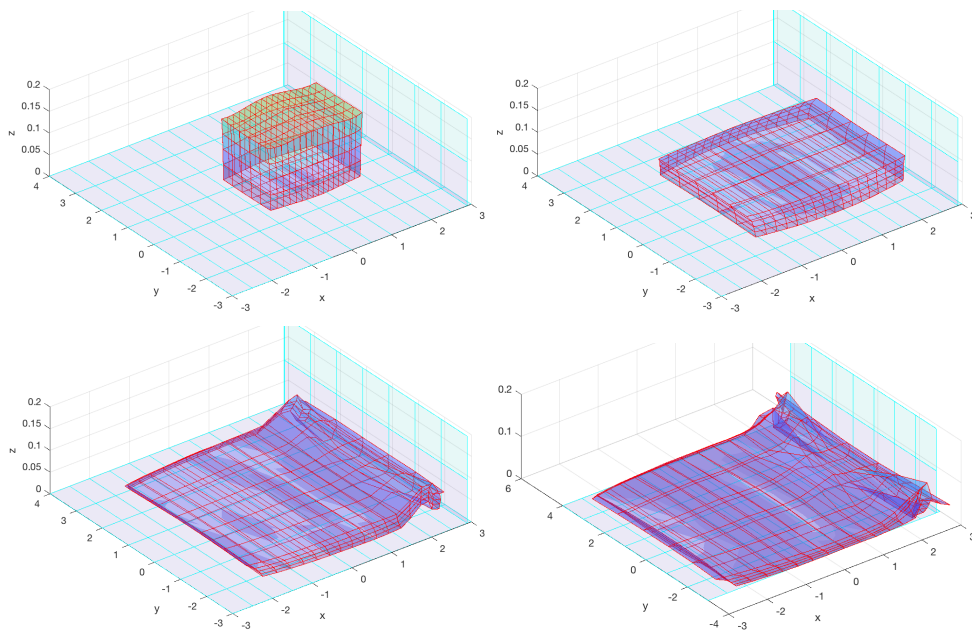


Figure 15: Barotropic fluid model with impact after 0.4s, 0.8s, 1.1s, 1.4s.

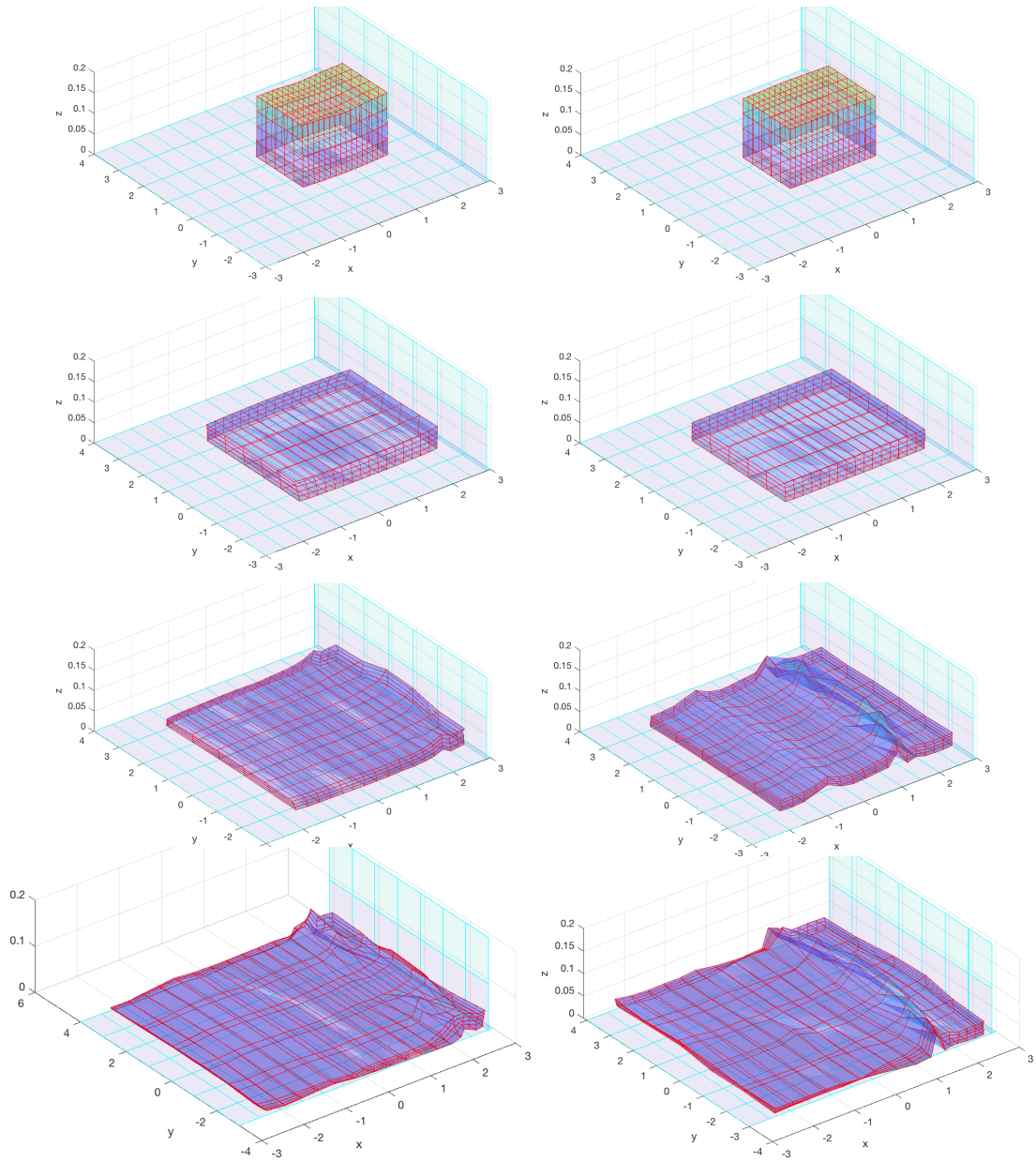


Figure 16: Fluid impact. *Left to right*: From less ($r = 10^8$) to more ($r = 10^9$) incompressibility. *Top to bottom*: after 0.4s, 0.8s, 1.1s, 1.4 s.

Note the large differences in behavior between the three tests that correspond to barotropic fluid (Fig. 15) and to fluids which are more or less incompressible (Fig. 16).

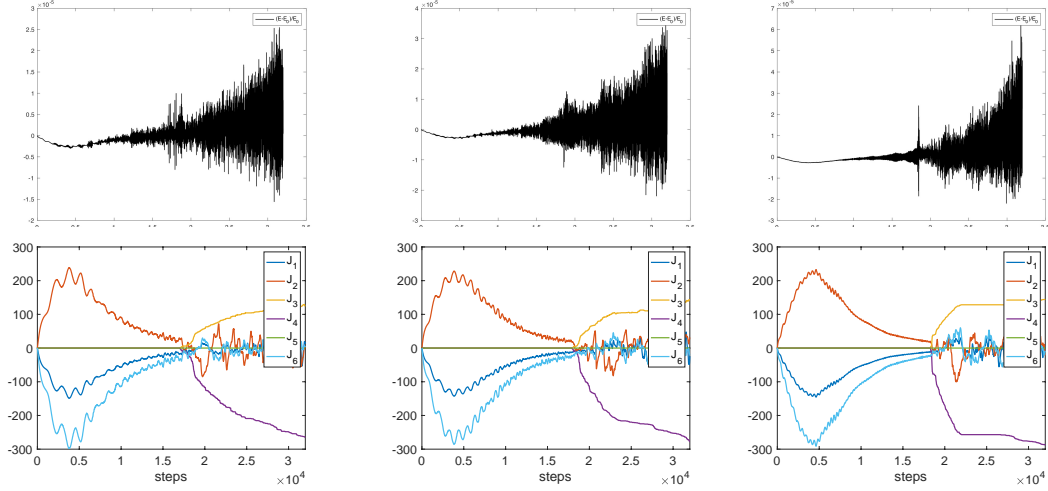


Figure 17: *From left to right:* Barotropic, incompressible ideal ($r = 10^8$), incompressible ideal ($r = 10^9$) fluid impact model. *From top to bottom:* Relative energy and momentum map evolution.

We observe that three components of the momentum map are preserved until the contact with the obstacle. These three components correspond to the symmetries of the gravitational term, given by the three dimensional subgroup of $SE(3)$ consisting of rotations around the vertical axis and translations in the horizontal plane. After contact only one symmetry with respect to one axis of translation is conserved, namely, the translation parallel to the obstacle wall. After impact, the total energy becomes more unstable, as observed in the 2D test, see Fig. 9.

Results concerning impact between fluid and solid are promising, however further investigations in numerics are necessary. In particular, we must develop an implicit integrator in order to increase the time-step and the performance of the integrator when the stability of the flow begin to be lost (e.g., when the flow is perturbed by the impact).

4.2.3 Convergence tests

Consider a barotropic fluid model with properties $\rho_0 = 997 \text{ kg/m}^3$, $\gamma = 6$, $A = \tilde{A}\rho_0^{-\gamma}$ with $\tilde{A} = 3.041 \times 10^4 \text{ Pa}$, and $B = 3.0397 \times 10^4 \text{ Pa}$. The size of the discrete reference configuration at time t^0 is $0.4 \text{ m} \times 0.4 \text{ m} \times 0.4 \text{ m}$. We consider the *explicit* integrator to study the convergence with respect to Δt and Δs_i , $i = 1, 2, 3$.

Barotropic fluid flowing freely over a surface. Given a fixed mesh, with values $\Delta s_1 = \Delta s_2 = \Delta s_3 = 0.1 \text{ m}$, we impose the gravity and one impenetrability constraint. We vary the time-steps as $\Delta t \in \{2.5 \times 10^{-4}, 1.25 \times 10^{-4}, 6.25 \times 10^{-5}, 3.125 \times 10^{-5}\}$. We compute the L^2 -errors in the position φ_d at time $t^N = 0.5 \text{ s}$, by comparing φ_d with an “exact solution” obtained with the time-step $\Delta t_{\text{ref}} = 7.8 \times 10^{-6} \text{ s}$. That is, for each value of Δt

we calculate

$$\|\varphi_d - \varphi_{\text{ref}}\|_{L^2} = \left(\sum_a \sum_b \sum_c \|\varphi_{a,b,c}^N - \varphi_{\text{ref};a,b,c}^N\|^2 \right)^{1/2}. \quad (72)$$

This yields the following convergence with respect to Δt

Δt	2.5×10^{-4}	1.25×10^{-4}	6.25×10^{-5}	3.125×10^{-5}
$\ \varphi_d - \varphi_{\text{ref}}\ _{L^2}$	9×10^{-3}	4.4×10^{-3}	2.1×10^{-3}	9.7×10^{-4}
rate		1.03	1.07	1.11

Given a fixed time-step $\Delta t = 3.125 \times 10^{-5}$, we vary the space-steps as $\Delta s_1 = \Delta s_2 = \Delta s_3 \in \{0.2, 0.1, 0.05, 0.025\}$. The “exact solution” is chosen with $\Delta s_{1;\text{ref}} = \Delta s_{2;\text{ref}} = \Delta s_{3;\text{ref}} = 0.0125\text{m}$. We compute the L^2 -errors in the position φ_d at time $t^N = 0.1\text{s}$. We get the following convergence with respect to $\Delta s_1 = \Delta s_2 = \Delta s_3$

$\Delta s_1 = \Delta s_2 = \Delta s_3$	0.2	0.1	0.05	0.025
$\ \varphi_d - \varphi_{\text{ref}}\ _{L^2}$	0.0753	0.0532	0.0269	0.0120
rate		0.5	0.98	1.16

An illustration of the test used for the numerical convergence is given in Fig. 18.

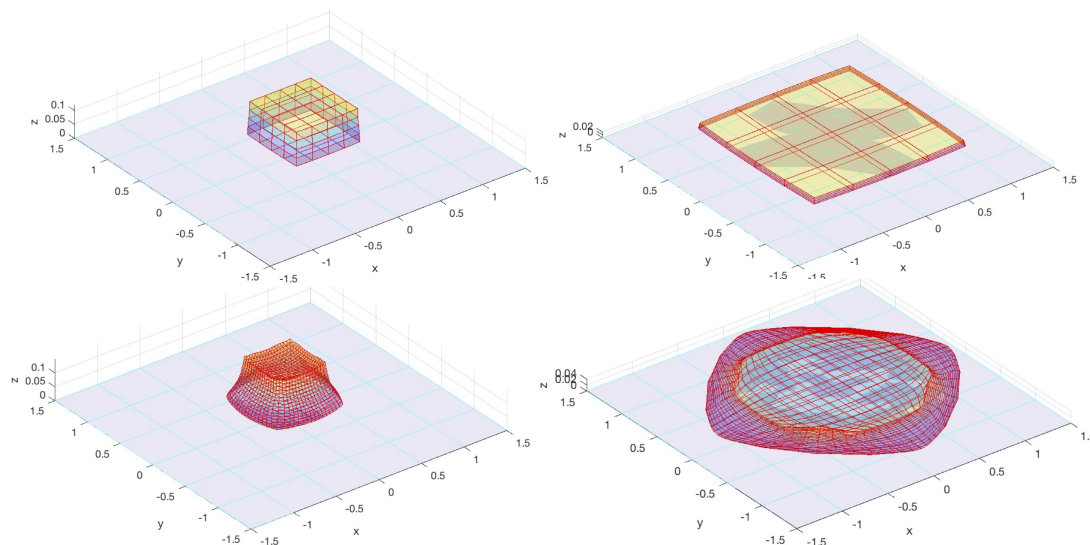


Figure 18: Barotropic fluid flowing freely over a surface with $\Delta t = 3.125 \times 10^{-5}$. From left to right: after 0.25s and 0.5s. From top to bottom: with $\Delta s_i = 0.1\text{m}$ and $\Delta s_i = 0.025\text{m}$.

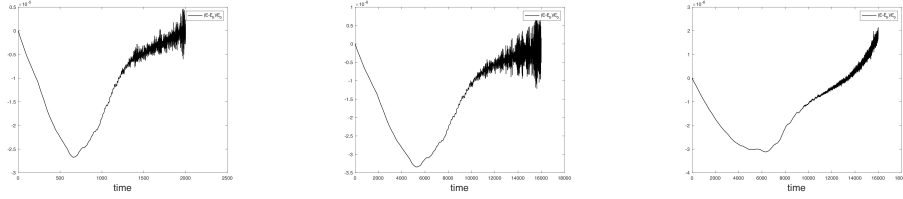


Figure 19: Relative error in the energy $(ET^j - ET^0)/ET^0$. From left to right: $(\Delta s_i = 0.1, \Delta t = 2.5 \times 10^{-4})$, $(\Delta s_i = 0.1, \Delta t = 3.125 \times 10^{-5})$, $(\Delta t = 3.125 \times 10^{-5}, \Delta s_i = 0.025)$.

5 Concluding remarks and future directions

This paper has presented new Lagrangian schemes for the regular motion of barotropic and incompressible fluid models, which preserve the momenta associated to symmetries, up to machine precision, and satisfy the nearly constant energy property of symplectic integrators, see Fig. 6 and 14. The schemes are derived by discretization of the geometric and variational structures underlying the spacetime formulation of continuum mechanics, seen as a particular instance of field theory. We have illustrated how this approach can naturally accommodate incompressibility and fluid impact against an obstacle by appropriately augmenting the discrete Lagrangian and thanks to our definition of the discrete Jacobian.

An important task for the future is the study of contacts, and of friction with heat exchange, between liquid and gas, which are important phenomena encountered for instance in ocean-atmosphere coupling.

Thanks to the clear link between the expressions of the discrete Jacobian and discrete gradient deformation in §3.1.2 & §4.1.2, see also [10], it is possible to treat the coupling of fluid and elasticity dynamics, based on appropriate variational formulations such as, for instance, those developed in [14, 19] for fluid-structure interaction.

The results in this paper also make it possible to further develop multisymplectic integrators to model flows interacting mightily with obstacles, which are problems commonly met in engineering and biological applications, for example, when rocks fall into the reservoir of a dam or with blood flow in arteries which impacts heart valves.

A Appendix

A.1 Derivatives of the discrete Lagrangian for 2D barotropic fluid

Explicit integrator: The partial derivatives of the discrete Lagrangian for a 2D barotropic fluid with internal energy $W(\rho_0, J)$ are listed below, where the discrete pressure at time t^j and spatial position ℓ , with the ordering $\ell = 1$ to $\ell = 4$ respectively associated to the nodes (j, a, b) , $(j, a + 1, b)$, $(j, a, b + 1)$, $(j, a + 1, b + 1)$, is defined as

$$P_\ell(\mathbb{Q}_{a,b}^j) = -\rho_0 \frac{\partial W(\mathbb{Q}_{a,b}^j)}{\partial J_\ell(\mathbb{Q}_{a,b}^j)} = P_W(\rho_0, J_\ell(\mathbb{Q}_{a,b}^j)).$$

For the special case of internal energy given in (9), we have

$$P_\ell(\mathbb{E}_{a,b}^j) = A \left(\frac{\rho_0}{J_\ell(\mathbb{E}_{a,b}^j)} \right)^\gamma - B. \quad (73)$$

$$\begin{aligned} A_{a,b}^j &= -\frac{M}{4}v_{a,b}^j + \frac{\Delta t}{4}P_1(\mathbb{E}_{a,b}^j) \left(\varphi_{a+1,b}^j - \varphi_{a,b+1}^j \right) \times \frac{\mathbf{n}_1(\mathbb{E}_{a,b}^j)}{|\mathbf{n}_1(\mathbb{E}_{a,b}^j)|} \\ &\quad + \frac{\Delta t}{4}P_2(\mathbb{E}_{a,b}^j) \left(\varphi_{a+1,b}^j - \varphi_{a+1,b+1}^j \right) \times \frac{\mathbf{n}_2(\mathbb{E}_{a,b}^j)}{|\mathbf{n}_2(\mathbb{E}_{a,b}^j)|} \\ &\quad + \frac{\Delta t}{4}P_3(\mathbb{E}_{a,b}^j) \left(\varphi_{a+1,b+1}^j - \varphi_{a,b+1}^j \right) \times \frac{\mathbf{n}_3(\mathbb{E}_{a,b}^j)}{|\mathbf{n}_3(\mathbb{E}_{a,b}^j)|} \end{aligned}$$

$$\begin{aligned} B_{a,b}^j &= -\frac{M}{4}v_{a+1,b}^j + \frac{\Delta t}{4}P_1(\mathbb{E}_{a,b}^j) \left(\varphi_{a,b+1}^j - \varphi_{a,b}^j \right) \times \frac{\mathbf{n}_1(\mathbb{E}_{a,b}^j)}{|\mathbf{n}_1(\mathbb{E}_{a,b}^j)|} \\ &\quad + \frac{\Delta t}{4}P_2(\mathbb{E}_{a,b}^j) \left(\varphi_{a+1,b+1}^j - \varphi_{a,b}^j \right) \times \frac{\mathbf{n}_2(\mathbb{E}_{a,b}^j)}{|\mathbf{n}_2(\mathbb{E}_{a,b}^j)|} \\ &\quad + \frac{\Delta t}{4}P_4(\mathbb{E}_{a,b}^j) \left(\varphi_{a+1,b+1}^j - \varphi_{a,b+1}^j \right) \times \frac{\mathbf{n}_4(\mathbb{E}_{a,b}^j)}{|\mathbf{n}_4(\mathbb{E}_{a,b}^j)|} \end{aligned}$$

$$\begin{aligned} C_{a,b}^j &= -\frac{M}{4}v_{a,b+1}^j + \frac{\Delta t}{4}P_1(\mathbb{E}_{a,b}^j) \left(\varphi_{a,b}^j - \varphi_{a+1,b}^j \right) \times \frac{\mathbf{n}_1(\mathbb{E}_{a,b}^j)}{|\mathbf{n}_1(\mathbb{E}_{a,b}^j)|} \\ &\quad + \frac{\Delta t}{4}P_3(\mathbb{E}_{a,b}^j) \left(\varphi_{a,b}^j - \varphi_{a+1,b+1}^j \right) \times \frac{\mathbf{n}_3(\mathbb{E}_{a,b}^j)}{|\mathbf{n}_3(\mathbb{E}_{a,b}^j)|} \\ &\quad + \frac{\Delta t}{4}P_4(\mathbb{E}_{a,b}^j) \left(\varphi_{a+1,b}^j - \varphi_{a+1,b+1}^j \right) \times \frac{\mathbf{n}_4(\mathbb{E}_{a,b}^j)}{|\mathbf{n}_4(\mathbb{E}_{a,b}^j)|} \end{aligned}$$

$$\begin{aligned} D_{a,b}^j &= -\frac{M}{4}v_{a+1,b+1}^j + \frac{\Delta t}{4}P_2(\mathbb{E}_{a,b}^j) \left(\varphi_{a,b}^j - \varphi_{a+1,b}^j \right) \times \frac{\mathbf{n}_2(\mathbb{E}_{a,b}^j)}{|\mathbf{n}_2(\mathbb{E}_{a,b}^j)|} \\ &\quad + \frac{\Delta t}{4}P_3(\mathbb{E}_{a,b}^j) \left(\varphi_{a,b+1}^j - \varphi_{a,b}^j \right) \times \frac{\mathbf{n}_3(\mathbb{E}_{a,b}^j)}{|\mathbf{n}_3(\mathbb{E}_{a,b}^j)|} \\ &\quad + \frac{\Delta t}{4}P_4(\mathbb{E}_{a,b}^j) \left(\varphi_{a,b+1}^j - \varphi_{a+1,b}^j \right) \times \frac{\mathbf{n}_4(\mathbb{E}_{a,b}^j)}{|\mathbf{n}_4(\mathbb{E}_{a,b}^j)|} \end{aligned}$$

with

$$\begin{aligned} \mathbf{n}_1(\mathbb{E}_{a,b}^j) &= (\varphi_{a+1,b}^j - \varphi_{a,b}^j) \times (\varphi_{a,b+1}^j - \varphi_{a,b}^j); \\ \mathbf{n}_2(\mathbb{E}_{a,b}^j) &= (\varphi_{a+1,b+1}^j - \varphi_{a+1,b}^j) \times (\varphi_{a,b}^j - \varphi_{a+1,b}^j); \\ \mathbf{n}_3(\mathbb{E}_{a,b}^j) &= (\varphi_{a,b}^j - \varphi_{a,b+1}^j) \times (\varphi_{a+1,b+1}^j - \varphi_{a,b+1}^j); \\ \mathbf{n}_4(\mathbb{E}_{a,b}^j) &= (\varphi_{a,b+1}^j - \varphi_{a+1,b+1}^j) \times (\varphi_{a+1,b}^j - \varphi_{a+1,b+1}^j). \end{aligned}$$

Implicit integrator: The partial derivatives of the Lagrangian for a 2D barotropic fluid with internal energy $W(\rho_0, J)$, discretized under the mid-point rules, are given by

$$\begin{aligned}\mathbb{A}_{a,b}^j &= \frac{\Delta t}{4^2} P_1(\mathbb{A}_{a,b}^j) \left((\varphi_{a+1,b}^j + \varphi_{a+1,b}^{j+1}) - (\varphi_{a,b+1}^j + \varphi_{a,b+1}^{j+1}) \right) \times \frac{\mathfrak{n}_1(\mathbb{A}_{a,b}^j)}{|\mathfrak{n}_1(\mathbb{A}_{a,b}^j)|} \\ &+ \frac{\Delta t}{4^2} P_2(\mathbb{A}_{a,b}^j) \left((\varphi_{a+1,b}^j + \varphi_{a+1,b}^{j+1}) - (\varphi_{a+1,b+1}^j + \varphi_{a+1,b+1}^{j+1}) \right) \times \frac{\mathfrak{n}_2(\mathbb{A}_{a,b}^j)}{|\mathfrak{n}_2(\mathbb{A}_{a,b}^j)|} \\ &+ \frac{\Delta t}{4^2} P_3(\mathbb{A}_{a,b}^j) \left((\varphi_{a+1,b+1}^j + \varphi_{a+1,b+1}^{j+1}) - (\varphi_{a,b+1}^j + \varphi_{a,b+1}^{j+1}) \right) \times \frac{\mathfrak{n}_3(\mathbb{A}_{a,b}^j)}{|\mathfrak{n}_3(\mathbb{A}_{a,b}^j)|}\end{aligned}$$

$$\begin{aligned}\mathbb{B}_{a,b}^j &= \frac{\Delta t}{4^2} P_1(\mathbb{B}_{a,b}^j) \left((\varphi_{a,b+1}^j + \varphi_{a,b+1}^{j+1}) - (\varphi_{a,b}^j + \varphi_{a,b}^{j+1}) \right) \times \frac{\mathfrak{n}_1(\mathbb{B}_{a,b}^j)}{|\mathfrak{n}_1(\mathbb{B}_{a,b}^j)|} \\ &+ \frac{\Delta t}{4^2} P_2(\mathbb{B}_{a,b}^j) \left((\varphi_{a+1,b+1}^j + \varphi_{a+1,b+1}^{j+1}) - (\varphi_{a,b}^j + \varphi_{a,b}^{j+1}) \right) \times \frac{\mathfrak{n}_2(\mathbb{B}_{a,b}^j)}{|\mathfrak{n}_2(\mathbb{B}_{a,b}^j)|} \\ &+ \frac{\Delta t}{4^2} P_4(\mathbb{B}_{a,b}^j) \left((\varphi_{a+1,b+1}^j + \varphi_{a+1,b+1}^{j+1}) - (\varphi_{a,b+1}^j + \varphi_{a,b+1}^{j+1}) \right) \times \frac{\mathfrak{n}_4(\mathbb{B}_{a,b}^j)}{|\mathfrak{n}_4(\mathbb{B}_{a,b}^j)|}\end{aligned}$$

$$\begin{aligned}\mathbb{C}_{a,b}^j &= \frac{\Delta t}{4^2} P_1(\mathbb{C}_{a,b}^j) \left((\varphi_{a,b}^j + \varphi_{a,b}^{j+1}) - (\varphi_{a+1,b}^j + \varphi_{a+1,b}^{j+1}) \right) \times \frac{\mathfrak{n}_1(\mathbb{C}_{a,b}^j)}{|\mathfrak{n}_1(\mathbb{C}_{a,b}^j)|} \\ &+ \frac{\Delta t}{4^2} P_3(\mathbb{C}_{a,b}^j) \left((\varphi_{a,b}^j + \varphi_{a,b}^{j+1}) - (\varphi_{a+1,b+1}^j + \varphi_{a+1,b+1}^{j+1}) \right) \times \frac{\mathfrak{n}_3(\mathbb{C}_{a,b}^j)}{|\mathfrak{n}_3(\mathbb{C}_{a,b}^j)|} \\ &+ \frac{\Delta t}{4^2} P_4(\mathbb{C}_{a,b}^j) \left((\varphi_{a+1,b}^j + \varphi_{a+1,b}^{j+1}) - (\varphi_{a+1,b+1}^j + \varphi_{a+1,b+1}^{j+1}) \right) \times \frac{\mathfrak{n}_4(\mathbb{C}_{a,b}^j)}{|\mathfrak{n}_4(\mathbb{C}_{a,b}^j)|}\end{aligned}$$

$$\begin{aligned}\mathbb{D}_{a,b}^j &= \frac{\Delta t}{4^2} P_2(\mathbb{D}_{a,b}^j) \left((\varphi_{a,b}^j + \varphi_{a,b}^{j+1}) - (\varphi_{a+1,b}^j + \varphi_{a+1,b}^{j+1}) \right) \times \frac{\mathfrak{n}_2(\mathbb{D}_{a,b}^j)}{|\mathfrak{n}_2(\mathbb{D}_{a,b}^j)|} \\ &+ \frac{\Delta t}{4^2} P_3(\mathbb{D}_{a,b}^j) \left((\varphi_{a,b+1}^j + \varphi_{a,b+1}^{j+1}) - (\varphi_{a,b}^j + \varphi_{a,b}^{j+1}) \right) \times \frac{\mathfrak{n}_3(\mathbb{D}_{a,b}^j)}{|\mathfrak{n}_3(\mathbb{D}_{a,b}^j)|} \\ &+ \frac{\Delta t}{4^2} P_4(\mathbb{D}_{a,b}^j) \left((\varphi_{a,b+1}^j + \varphi_{a,b+1}^{j+1}) - (\varphi_{a+1,b}^j + \varphi_{a+1,b}^{j+1}) \right) \times \frac{\mathfrak{n}_4(\mathbb{D}_{a,b}^j)}{|\mathfrak{n}_4(\mathbb{D}_{a,b}^j)|}\end{aligned}$$

with

$$\begin{aligned}\mathfrak{n}_1(\mathbb{A}_{a,b}^j) &= \left((\varphi_{a+1,b}^j + \varphi_{a+1,b}^{j+1}) - (\varphi_{a,b}^j + \varphi_{a,b}^{j+1}) \right) \times \left((\varphi_{a,b+1}^j + \varphi_{a,b+1}^{j+1}) - (\varphi_{a,b}^j + \varphi_{a,b}^{j+1}) \right); \\ \mathfrak{n}_2(\mathbb{A}_{a,b}^j) &= \left((\varphi_{a+1,b+1}^j + \varphi_{a+1,b+1}^{j+1}) - (\varphi_{a+1,b}^j + \varphi_{a+1,b}^{j+1}) \right) \times \left((\varphi_{a,b}^j + \varphi_{a,b}^{j+1}) - (\varphi_{a+1,b}^j + \varphi_{a+1,b}^{j+1}) \right); \\ \mathfrak{n}_3(\mathbb{A}_{a,b}^j) &= \left((\varphi_{a,b}^j + \varphi_{a,b}^{j+1}) - (\varphi_{a,b+1}^j + \varphi_{a,b+1}^{j+1}) \right) \times \left((\varphi_{a+1,b+1}^j + \varphi_{a+1,b+1}^{j+1}) - (\varphi_{a,b+1}^j + \varphi_{a,b+1}^{j+1}) \right); \\ \mathfrak{n}_4(\mathbb{A}_{a,b}^j) &= \left((\varphi_{a,b+1}^j + \varphi_{a,b+1}^{j+1}) - (\varphi_{a+1,b+1}^j + \varphi_{a+1,b+1}^{j+1}) \right) \times \left((\varphi_{a+1,b}^j + \varphi_{a+1,b}^{j+1}) - (\varphi_{a+1,b+1}^j + \varphi_{a+1,b+1}^{j+1}) \right).\end{aligned}$$

Where the pressures $P_\ell(\mathbb{A}_{a,b}^j)$, $\ell = 1, 2, 3, 4$, were defined in (73).

A.2 Discrete Euler-Lagrange equations for 2D barotropic fluid

$$\begin{aligned}
\rho_0 \left(\frac{v_{a,b}^j - v_{a,b}^{j-1}}{\Delta t} \right) = \frac{1}{4\Delta s_1 \Delta s_2} \left\{ - \left(P_1(\mathbb{P}_{a,b}^j) \left(\varphi_{a,b+1}^j - \varphi_{a+1,b}^j \right) \times \frac{\mathbf{n}_1(\mathbb{P}_{a,b}^j)}{|\mathbf{n}_1(\mathbb{P}_{a,b}^j)|} \right. \right. \\
+ P_2(\mathbb{P}_{a-1,b}^j) \left(\varphi_{a-1,b}^j - \varphi_{a,b+1}^j \right) \times \frac{\mathbf{n}_2(\mathbb{P}_{a-1,b}^j)}{|\mathbf{n}_2(\mathbb{P}_{a-1,b}^j)|} \\
+ P_3(\mathbb{P}_{a,b-1}^j) \left(\varphi_{a+1,b}^j - \varphi_{a,b-1}^j \right) \times \frac{\mathbf{n}_3(\mathbb{P}_{a,b-1}^j)}{|\mathbf{n}_3(\mathbb{P}_{a,b-1}^j)|} \\
+ P_4(\mathbb{P}_{a-1,b-1}^j) \left(\varphi_{a,b-1}^j - \varphi_{a-1,b}^j \right) \times \frac{\mathbf{n}_4(\mathbb{P}_{a-1,b-1}^j)}{|\mathbf{n}_4(\mathbb{P}_{a-1,b-1}^j)|} \Bigg) \\
+ \left(P_2(\mathbb{P}_{a,b}^j) \left(\varphi_{a+1,b}^j - \varphi_{a+1,b+1}^j \right) \times \frac{\mathbf{n}_2(\mathbb{P}_{a,b}^j)}{|\mathbf{n}_2(\mathbb{P}_{a,b}^j)|} \right. \\
+ P_4(\mathbb{P}_{a,b-1}^j) \left(\varphi_{a+1,b-1}^j - \varphi_{a+1,b}^j \right) \times \frac{\mathbf{n}_4(\mathbb{P}_{a,b-1}^j)}{|\mathbf{n}_4(\mathbb{P}_{a,b-1}^j)|} \Bigg) \\
+ \left(P_3(\mathbb{P}_{a,b}^j) \left(\varphi_{a+1,b+1}^j - \varphi_{a,b+1}^j \right) \times \frac{\mathbf{n}_3(\mathbb{P}_{a,b}^j)}{|\mathbf{n}_3(\mathbb{P}_{a,b}^j)|} \right. \\
+ P_4(\mathbb{P}_{a-1,b}^j) \left(\varphi_{a,b+1}^j - \varphi_{a-1,b+1}^j \right) \times \frac{\mathbf{n}_4(\mathbb{P}_{a-1,b}^j)}{|\mathbf{n}_4(\mathbb{P}_{a-1,b}^j)|} \Bigg) \\
+ \left(P_1(\mathbb{P}_{a-1,b}^j) \left(\varphi_{a-1,b+1}^j - \varphi_{a-1,b}^j \right) \times \frac{\mathbf{n}_1(\mathbb{P}_{a-1,b}^j)}{|\mathbf{n}_1(\mathbb{P}_{a-1,b}^j)|} \right. \\
+ P_3(\mathbb{P}_{a-1,b-1}^j) \left(\varphi_{a-1,b}^j - \varphi_{a-1,b-1}^j \right) \times \frac{\mathbf{n}_3(\mathbb{P}_{a-1,b-1}^j)}{|\mathbf{n}_3(\mathbb{P}_{a-1,b-1}^j)|} \Bigg) \\
+ \left(P_2(\mathbb{P}_{a-1,b-1}^j) \left(\varphi_{a-1,b-1}^j - \varphi_{a,b-1}^j \right) \times \frac{\mathbf{n}_2(\mathbb{P}_{a-1,b-1}^j)}{|\mathbf{n}_2(\mathbb{P}_{a-1,b-1}^j)|} \right. \\
+ P_1(\mathbb{P}_{a,b-1}^j) \left(\varphi_{a,b-1}^j - \varphi_{a+1,b-1}^j \right) \times \frac{\mathbf{n}_1(\mathbb{P}_{a,b-1}^j)}{|\mathbf{n}_1(\mathbb{P}_{a,b-1}^j)|} \Bigg) \Bigg\}
\end{aligned}$$

Interpretation of the discrete Euler-Lagrange equations: *discrete balance of momentum*

$$\rho_0(v^j - v^{j-1})/\Delta t = -[(P_{\text{ext}} \cdot L_{\text{ext}})\mathbf{n}_{\text{ext}} - (P_{\text{int}} \cdot L_{\text{int}})\mathbf{n}_{\text{int}}]_j / \text{area},$$

where \mathbf{n}_{ext} , \mathbf{n}_{int} are unit vectors that point outward of the boundaries.

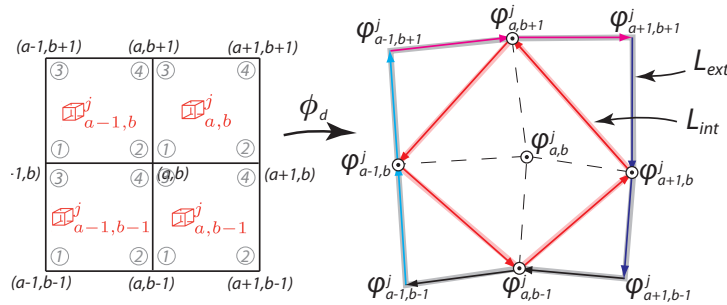


Figure 20: Internal and external lengths L_{int} , L_{ext} .

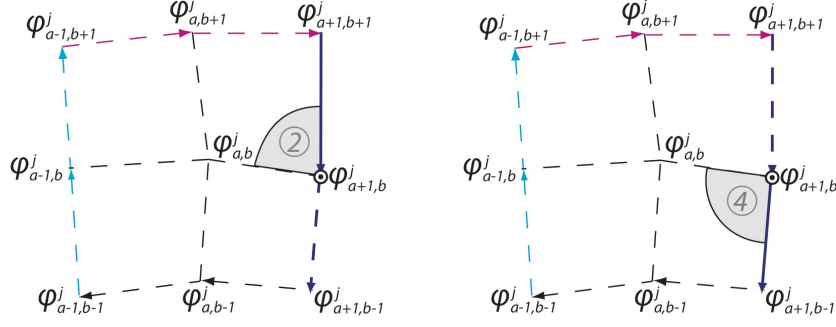


Figure 21: On the left: the force $P_2(\mathbb{E}_{a,b}^j) (\varphi_{a+1,b}^j - \varphi_{a+1,b+1}^j) \times \frac{\mathbf{n}_2(\mathbb{E}_{a,b}^j)}{|\mathbf{n}_2(\mathbb{E}_{a,b}^j)|}$ associated to the pressure $P_2(\mathbb{E}_{a,b}^j)$ and the length $|\varphi_{a+1,b}^j - \varphi_{a+1,b+1}^j|$. On the right $P_4(\mathbb{E}_{a,b-1}^j) (\varphi_{a+1,b-1}^j - \varphi_{a+1,b}^j) \times \frac{\mathbf{n}_4(\mathbb{E}_{a,b-1}^j)}{|\mathbf{n}_4(\mathbb{E}_{a,b-1}^j)|}$ associated to the pressure $P_4(\mathbb{E}_{a,b-1}^j)$ and the length $|\varphi_{a+1,b-1}^j - \varphi_{a+1,b}^j|$.

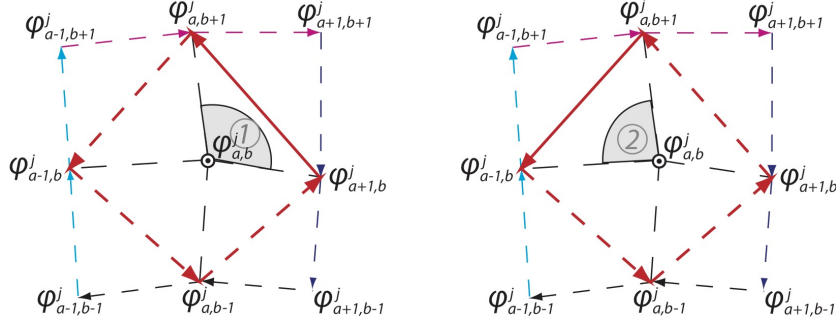


Figure 22: On the left: the force $P_1(\mathbb{E}_{a,b}^j) (\varphi_{a,b+1}^j - \varphi_{a+1,b}^j) \times \frac{\mathbf{n}_1(\mathbb{E}_{a,b}^j)}{|\mathbf{n}_1(\mathbb{E}_{a,b}^j)|}$ associated to the pressure $P_1(\mathbb{E}_{a,b}^j)$ and the length $|\varphi_{a,b+1}^j - \varphi_{a+1,b}^j|$. On the right $P_2(\mathbb{E}_{a-1,b}^j) (\varphi_{a-1,b}^j - \varphi_{a,b+1}^j) \times \frac{\mathbf{n}_2(\mathbb{E}_{a-1,b}^j)}{|\mathbf{n}_2(\mathbb{E}_{a-1,b}^j)|}$ associated to the pressure $P_2(\mathbb{E}_{a-1,b}^j)$ and the length $|\varphi_{a-1,b}^j - \varphi_{a,b+1}^j|$.

A.3 Discrete Jacobian on $\mathbb{E}_{a,b,c}^j$ in 3D

$$\begin{aligned}
 J_2(\mathbb{E}_{a,b,c}^j) &= (\mathbf{F}_{2;a+1,b,c}^j \times \mathbf{F}_{4;a+1,b,c}^j) \cdot \mathbf{F}_{3;a+1,b,c}^j, & J_5(\mathbb{E}_{a,b,c}^j) &= (\mathbf{F}_{4;a+1,b+1,c}^j \times \mathbf{F}_{5;a+1,b+1,c}^j) \cdot \mathbf{F}_{3;a+1,b+1,c}^j \\
 J_3(\mathbb{E}_{a,b,c}^j) &= (\mathbf{F}_{5;a,b+1,c}^j \times \mathbf{F}_{1;a,b+1,c}^j) \cdot \mathbf{F}_{3;a,b+1,c}^j, & J_6(\mathbb{E}_{a,b,c}^j) &= (\mathbf{F}_{1;a,b+1,c+1}^j \times \mathbf{F}_{5;a,b+1,c+1}^j) \cdot \mathbf{F}_{6;a,b+1,c+1}^j \\
 J_4(\mathbb{E}_{a,b,c}^j) &= (\mathbf{F}_{2;a,b,c+1}^j \times \mathbf{F}_{1;a,b,c+1}^j) \cdot \mathbf{F}_{6;a,b,c+1}^j, & J_7(\mathbb{E}_{a,b,c}^j) &= (\mathbf{F}_{4;a+1,b,c+1}^j \times \mathbf{F}_{2;a+1,b,c+1}^j) \cdot \mathbf{F}_{6;a+1,b,c+1}^j \\
 J_8(\mathbb{E}_{a,b,c}^j) &= (\mathbf{F}_{5;a+1,b+1,c+1}^j \times \mathbf{F}_{4;a+1,b+1,c+1}^j) \cdot \mathbf{F}_{6;a+1,b+1,c+1}^j.
 \end{aligned}$$

A.4 Derivatives of the discrete Lagrangian for 3D barotropic fluid

With the same definition as in §A.1, the partial derivatives of the discrete Lagrangian for a 3D barotropic fluid with internal energy $W(\rho_0, J)$ are listed below.

$$\begin{aligned}
A_{a,b,c}^j &= -\frac{M}{8}v_{a,b,c}^j + \frac{\Delta t}{8} \left\{ -P_1 \left(\mathbf{n}_1^{(12)} + \mathbf{n}_1^{(23)} + \mathbf{n}_1^{(31)} \right) + P_4 \mathbf{n}_4^{(12)} + P_3 \mathbf{n}_3^{(23)} + P_2 \mathbf{n}_2^{(31)} \right\} (\mathbb{E}_{a,b,c}^j), \\
B_{a,b,c}^j &= -\frac{M}{8}v_{a+1,b,c}^j + \frac{\Delta t}{8} \left\{ -P_2 \left(\mathbf{n}_2^{(12)} + \mathbf{n}_2^{(23)} + \mathbf{n}_2^{(31)} \right) + P_7 \mathbf{n}_7^{(12)} + P_1 \mathbf{n}_1^{(23)} + P_5 \mathbf{n}_5^{(31)} \right\} (\mathbb{E}_{a,b,c}^j), \\
C_{a,b,c}^j &= -\frac{M}{8}v_{a,b+1,c}^j + \frac{\Delta t}{8} \left\{ -P_3 \left(\mathbf{n}_3^{(12)} + \mathbf{n}_3^{(23)} + \mathbf{n}_3^{(31)} \right) + P_6 \mathbf{n}_6^{(12)} + P_5 \mathbf{n}_5^{(23)} + P_1 \mathbf{n}_1^{(31)} \right\} (\mathbb{E}_{a,b,c}^j), \\
D_{a,b,c}^j &= -\frac{M}{8}v_{a,b,c+1}^j + \frac{\Delta t}{8} \left\{ -P_4 \left(\mathbf{n}_4^{(12)} + \mathbf{n}_4^{(23)} + \mathbf{n}_4^{(31)} \right) + P_1 \mathbf{n}_1^{(12)} + P_7 \mathbf{n}_7^{(23)} + P_6 \mathbf{n}_6^{(31)} \right\} (\mathbb{E}_{a,b,c}^j), \\
E_{a,b,c}^j &= -\frac{M}{8}v_{a+1,b+1,c}^j + \frac{\Delta t}{8} \left\{ -P_5 \left(\mathbf{n}_5^{(12)} + \mathbf{n}_5^{(23)} + \mathbf{n}_5^{(31)} \right) + P_8 \mathbf{n}_8^{(12)} + P_2 \mathbf{n}_2^{(23)} + P_3 \mathbf{n}_3^{(31)} \right\} (\mathbb{E}_{a,b,c}^j), \\
F_{a,b,c}^j &= -\frac{M}{8}v_{a,b+1,c+1}^j + \frac{\Delta t}{8} \left\{ -P_6 \left(\mathbf{n}_6^{(12)} + \mathbf{n}_6^{(23)} + \mathbf{n}_6^{(31)} \right) + P_3 \mathbf{n}_3^{(12)} + P_4 \mathbf{n}_4^{(23)} + P_8 \mathbf{n}_8^{(31)} \right\} (\mathbb{E}_{a,b,c}^j), \\
G_{a,b,c}^j &= -\frac{M}{8}v_{a+1,b,c+1}^j + \frac{\Delta t}{8} \left\{ -P_7 \left(\mathbf{n}_7^{(12)} + \mathbf{n}_7^{(23)} + \mathbf{n}_7^{(31)} \right) + P_2 \mathbf{n}_2^{(12)} + P_8 \mathbf{n}_8^{(23)} + P_4 \mathbf{n}_4^{(31)} \right\} (\mathbb{E}_{a,b,c}^j), \\
H_{a,b,c}^j &= -\frac{M}{8}v_{a+1,b+1,c+1}^j + \frac{\Delta t}{8} \left\{ -P_8 \left(\mathbf{n}_8^{(12)} + \mathbf{n}_8^{(23)} + \mathbf{n}_8^{(31)} \right) + P_5 \mathbf{n}_5^{(12)} + P_6 \mathbf{n}_6^{(23)} + P_7 \mathbf{n}_7^{(31)} \right\} (\mathbb{E}_{a,b,c}^j),
\end{aligned}$$

where

$$\begin{aligned}
\mathbf{n}_1(\mathbb{E}_{a,b,c}^j) &= ((\varphi_{a+1,b,c}^j - \varphi_{a,b,c}^j) \times (\varphi_{a,b+1,c}^j - \varphi_{a,b,c}^j)) \cdot (\varphi_{a,b,c+1}^j - \varphi_{a,b,c}^j), \\
\mathbf{n}_2(\mathbb{E}_{a,b,c}^j) &= ((\varphi_{a+1,b+1,c}^j - \varphi_{a+1,b,c}^j) \times (\varphi_{a,b,c}^j - \varphi_{a+1,b,c}^j)) \cdot (\varphi_{a+1,b,c+1}^j - \varphi_{a+1,b,c}^j), \\
\mathbf{n}_3(\mathbb{E}_{a,b,c}^j) &= ((\varphi_{a,b,c}^j - \varphi_{a,b+1,c}^j) \times (\varphi_{a+1,b+1,c}^j - \varphi_{a,b+1,c}^j)) \cdot (\varphi_{a,b+1,c+1}^j - \varphi_{a,b+1,c}^j), \\
\mathbf{n}_4(\mathbb{E}_{a,b,c}^j) &= ((\varphi_{a,b+1,c+1}^j - \varphi_{a,b,c+1}^j) \times (\varphi_{a+1,b,c+1}^j - \varphi_{a,b,c+1}^j)) \cdot (\varphi_{a,b,c}^j - \varphi_{a,b,c+1}^j), \\
\mathbf{n}_5(\mathbb{E}_{a,b,c}^j) &= ((\varphi_{a,b+1,c}^j - \varphi_{a+1,b+1,c}^j) \times (\varphi_{a+1,b,c}^j - \varphi_{a+1,b+1,c}^j)) \cdot (\varphi_{a+1,b+1,c+1}^j - \varphi_{a+1,b+1,c}^j), \\
\mathbf{n}_6(\mathbb{E}_{a,b,c}^j) &= ((\varphi_{a+1,b+1,c+1}^j - \varphi_{a,b+1,c+1}^j) \times (\varphi_{a,b,c+1}^j - \varphi_{a,b+1,c+1}^j)) \cdot (\varphi_{a,b+1,c}^j - \varphi_{a,b+1,c+1}^j), \\
\mathbf{n}_7(\mathbb{E}_{a,b,c}^j) &= ((\varphi_{a,b,c+1}^j - \varphi_{a+1,b,c+1}^j) \times (\varphi_{a+1,b+1,c+1}^j - \varphi_{a+1,b,c+1}^j)) \cdot (\varphi_{a+1,b,c}^j - \varphi_{a+1,b,c+1}^j), \\
\mathbf{n}_8(\mathbb{E}_{a,b,c}^j) &= ((\varphi_{a+1,b,c+1}^j - \varphi_{a+1,b+1,c+1}^j) \times (\varphi_{a,b+1,c+1}^j - \varphi_{a+1,b+1,c+1}^j)) \cdot (\varphi_{a+1,b+1,c}^j - \varphi_{a+1,b+1,c+1}^j),
\end{aligned}$$

and

$$\begin{aligned}
\mathbf{n}_1^{(12)} &= (\varphi_{a+1,b,c}^j - \varphi_{a,b,c}^j) \times (\varphi_{a,b+1,c}^j - \varphi_{a,b,c}^j), \\
\mathbf{n}_1^{(23)} &= (\varphi_{a,b+1,c}^j - \varphi_{a,b,c}^j) \times (\varphi_{a,b,c+1}^j - \varphi_{a,b,c}^j), \\
\mathbf{n}_1^{(31)} &= (\varphi_{a,b,c+1}^j - \varphi_{a,b,c}^j) \times (\varphi_{a+1,b,c}^j - \varphi_{a,b,c}^j), \\
J_1(\mathbb{E}_{a,b,c}^j) &= \frac{((\varphi_{a+1,b,c}^j - \varphi_{a,b,c}^j) \times (\varphi_{a,b+1,c}^j - \varphi_{a,b,c}^j)) \cdot (\varphi_{a,b,c+1}^j - \varphi_{a,b,c}^j)}{|s_{a+1,b,c} - s_{a,b,c}| |s_{a,b+1,c} - s_{a,b,c}| |s_{a,b,c+1} - s_{a,b,c}|}.
\end{aligned}$$

Note that in $\mathbf{n}_1^{(12)}$, $\mathbf{n}_1^{(23)}$, $\mathbf{n}_1^{(31)}$ we adopt the usual expressions (12), (23), (31) for permutation of the elements of the set $\{(\varphi_{a+1,b,c}^j - \varphi_{a,b,c}^j), (\varphi_{a,b+1,c}^j - \varphi_{a,b,c}^j), (\varphi_{a,b,c+1}^j - \varphi_{a,b,c}^j)\}$ which compose \mathbf{n}_1 .

A.5 Discrete Euler-Lagrange equations for 3D barotropic fluid

$$\begin{aligned}
\rho_0 \left(\frac{v_{a,b,c}^j - v_{a,b,c}^{j-1}}{\Delta t} \right) = & \frac{1}{8\Delta s_1 \Delta s_2 \Delta s_3} \left\{ -P_1 \left(\mathbf{n}_1^{(12)} + \mathbf{n}_1^{(23)} + \mathbf{n}_1^{(31)} \right) (\mathbb{E}_{a,b,c}^j) \right. \\
& - P_2 \left(\mathbf{n}_2^{(12)} + \mathbf{n}_2^{(23)} + \mathbf{n}_2^{(31)} \right) (\mathbb{E}_{a-1,b,c}^j) - P_3 \left(\mathbf{n}_3^{(12)} + \mathbf{n}_3^{(23)} + \mathbf{n}_3^{(31)} \right) (\mathbb{E}_{a,b-1,c}^j) \\
& - P_4 \left(\mathbf{n}_4^{(12)} + \mathbf{n}_4^{(23)} + \mathbf{n}_4^{(31)} \right) (\mathbb{E}_{a,b,c-1}^j) - P_5 \left(\mathbf{n}_5^{(12)} + \mathbf{n}_5^{(23)} + \mathbf{n}_5^{(31)} \right) (\mathbb{E}_{a-1,b-1,c}^j) \\
& - P_6 \left(\mathbf{n}_6^{(12)} + \mathbf{n}_6^{(23)} + \mathbf{n}_6^{(31)} \right) (\mathbb{E}_{a,b-1,c-1}^j) - P_7 \left(\mathbf{n}_7^{(12)} + \mathbf{n}_7^{(23)} + \mathbf{n}_7^{(31)} \right) (\mathbb{E}_{a-1,b,c-1}^j) \\
& - P_8 \left(\mathbf{n}_8^{(12)} + \mathbf{n}_8^{(23)} + \mathbf{n}_8^{(31)} \right) (\mathbb{E}_{a-1,b-1,c-1}^j) \\
& + \left(P_4 \mathbf{n}_4^{(12)} + P_3 \mathbf{n}_3^{(23)} + P_2 \mathbf{n}_2^{(31)} \right) (\mathbb{E}_{a,b,c}^j) \\
& + \left(P_7 \mathbf{n}_7^{(12)} + P_1 \mathbf{n}_1^{(23)} + P_5 \mathbf{n}_5^{(31)} \right) (\mathbb{E}_{a-1,b,c}^j) \\
& + \left(P_6 \mathbf{n}_6^{(12)} + P_5 \mathbf{n}_5^{(23)} + P_1 \mathbf{n}_1^{(31)} \right) (\mathbb{E}_{a,b-1,c}^j) \\
& + \left(P_1 \mathbf{n}_1^{(12)} + P_7 \mathbf{n}_7^{(23)} + P_6 \mathbf{n}_6^{(31)} \right) (\mathbb{E}_{a,b,c-1}^j) \\
& + \left(P_8 \mathbf{n}_8^{(12)} + P_2 \mathbf{n}_2^{(23)} + P_3 \mathbf{n}_3^{(31)} \right) (\mathbb{E}_{a-1,b-1,c}^j) \\
& + \left(P_3 \mathbf{n}_3^{(12)} + P_4 \mathbf{n}_4^{(23)} + P_8 \mathbf{n}_8^{(31)} \right) (\mathbb{E}_{a,b-1,c-1}^j) \\
& + \left(P_2 \mathbf{n}_2^{(12)} + P_8 \mathbf{n}_8^{(23)} + P_4 \mathbf{n}_4^{(31)} \right) (\mathbb{E}_{a-1,b,c-1}^j) \\
& \left. + \left(P_5 \mathbf{n}_5^{(12)} + P_6 \mathbf{n}_6^{(23)} + P_7 \mathbf{n}_7^{(31)} \right) (\mathbb{E}_{a-1,b-1,c-1}^j) \right\}
\end{aligned}$$

Interpretation of the discrete Euler-Lagrange equations: *discrete balance of momentum*

$$\rho_0 (v^j - v^{j-1}) / \Delta t = - [(P_{\text{ext}} \cdot S_{\text{ext}}) \mathbf{n}_{\text{ext}} - (P_{\text{int}} \cdot S_{\text{int}}) \mathbf{n}_{\text{int}}]_j / \text{volume}.$$

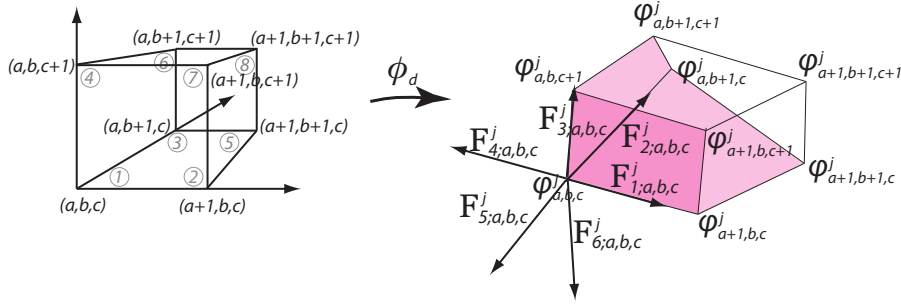


Figure 23: In red: the internal surfaces S_{int} associated to the cell $\mathbb{E}_{a,b,c}^j$.

References

- [1] Bauer, W. and Gay-Balmaz, F. [2019], Towards a geometric variational discretization of compressible fluids: the rotating shallow water equations, *J. Comp. Dyn.*, **16**(1), 1–37.
- [2] Bazaraa, M.S., Sherali, H.D., and Shetty, C.M. [2006] *Nonlinear programming: Theory and Algorithms*, Wiley, 2006.

- [3] Bridges, T. and Reich, S. [2001], Multi-symplectic integrators: numerical schemes for Hamiltonian PDEs that conserve symplecticity, *Phys. Lett. A* **284**(4-5), 184–193.
- [4] Chorin, A.J. and Marsden, J. E. [1990], *A Mathematical Introduction to Fluid Dynamics*. Springer.
- [5] Courant R. and Friedrichs K. O. [1948], *Supersonic Flow and Shock Waves*, Institute for mathematics and mechanics, New York University, New-York, 1948.
- [6] Demoures, F., Gay-Balmaz, F., Desbrun, M., Ratiu, T. S., and Alejandro, A. [2017], A multisymplectic integrator for elastodynamic frictionless impact problems, *Comput. Methods in Appl. Mech. Eng.*, **315**, 1025–1052.
- [7] Demoures, F., Gay-Balmaz, F., Kobilarov, M. and Ratiu T. S. [2014], Multisymplectic Lie group variational integrators for a geometrically exact beam in \mathbb{R}^3 , *Commun. Nonlinear Sci. Numer. Simulat.*, **19**(10), 3492–3512.
- [8] Demoures, F., Gay-Balmaz, F., and Ratiu, T. S. [2014], Multisymplectic variational integrator and space/time symplecticity, *Anal. Appl.*, **14**(3), 341–391.
- [9] Demoures, F., Gay-Balmaz, F., and Ratiu, T. S. [2016], Multisymplectic variational integrators for nonsmooth Lagrangian continuum mechanics, *Forum Math. Sigma*, **4**, e19, 54p.
- [10] Demoures, F. [2019], Multisymplectic variational integrators and constitutive discrete theory of elasticity, submitted.
- [11] Donea J, Giuliani S, Halleux J. P. [1982], An arbitrary Lagrangian-Eulerian finite element method for transient dynamic fluid-structure interactions, *Comput. Meth. in Appl. Mech. Eng.*, **33**, 689–723.
- [12] Donea, J. [1983], Arbitrary Lagrangian-Eulerian finite element methods. In T. Belytschko and T. J. R. Hughes, editors, *Computational Methods in Transient Analysis*, Elsevier.
- [13] Farhat, C., Rallu, A., Wang, K., and Belytschko, T. [2010], Robust and provably second-order explicit-explicit and implicit-explicit staggered time-integrators for highly non-linear compressible fluid-structure interaction problems, *Int. J. Numer. Meth. Eng.*, **84**, 73–107.
- [14] Farkhutdinov, T., F. Gay-Balmaz, and V. Putkaradze [2020], Geometric variational approach to the dynamics of porous media filled with incompressible fluid, *Acta Mechanica*, **431**(9), 3897–3924. <https://arxiv.org/pdf/2007.02605.pdf>
- [15] Fetecau R.C., Marsden J.E., and West M. [2003], Variational multisymplectic formulations of nonsmooth continuum mechanics, in *Perspectives and Problems in Nonlinear Science*, 229–261, Springer, New York, 2003.
- [16] Gawlik, E. S. and Gay-Balmaz, F. [2020], A variational finite element discretization of compressible flow, *Found. Comput. Math.*, 1-41. <https://arxiv.org/pdf/1910.05648.pdf>
- [17] Gay-Balmaz, F., Marsden, J. E. Ratiu, T. S. [2012], Reduced variational formulations in free boundary continuum mechanics, *J. Nonlin. Sci.*, **22**(4), 463–497.
- [18] Gotay, M. J., J. Isenberg, J. E. Marsden, R. Montgomery, J. Sniatycki, P. B. Yasskin [1997], Momentum maps and classical fields. Part I: Covariant field theory, (1997), [arXiv:physics/9801019v2](https://arxiv.org/abs/physics/9801019v2).
- [19] Gay-Balmaz, F. and V. Putkaradze [2020], Variational methods for fluid-structure interactions, in *Springer Handbook of Variational Methods for Nonlinear Geometric Data*, 175–205, Springer.
- [20] Hughes, T. J. R., Liu, W. K., Zimmerman, T. [1981], Lagrangian-Eulerian finite element formulation for incompressible viscous flow, *Comput. Meth. in Appl. Mech. Eng.*, **29**, 329–49.
- [21] Lew, A., Marsden, J. E., Ortiz, M., and West, M. [2003], Asynchronous variational integrators, *Arch. Rational Mech. Anal.*, **167**(2), 85–146.
- [22] Lew, A., Marsden, J. E., Ortiz, M., and West, M. [2004], Variational time integrators, *Internat. J. Numer. Methods Eng.*, **60**(1), 153–212.
- [23] Marsden, J. E. and Hughes, T. J. R. *Mathematical Foundations of Elasticity*. Prentice-Hall, 1983.

- [24] Marsden, J. E., Patrick, G. W., and Shkoller, S. [1998], Multisymplectic geometry, variational integrators and nonlinear PDEs, *Comm. Math. Phys.*, **199**, 351–395.
- [25] Marsden, J. E., Pekarsky, S. Shkoller, S., and West, M. [2001], Variational Methods, Multisymplectic Geometry and Continuum Mechanics, *J. Geom. Phys.*, **38**, 253-284.
- [26] Marsden, J. E. and West M. [2001], Discrete mechanics and variational integrators, *Acta Numer.* **10**, 357–514.
- [27] Masud, A., Hughes, T. J. R. [1997], A space-time Galerkin/Least squares finite element formulation of the Navier-Stokes equations for moving domain problems, *Comput. Meth. in Appl. Mech. Eng.*, **146**, 91–126.
- [28] Moreau, J.-J. [1973], *On Unilateral Constraints, Friction and Plasticity*, C.I.M.E. Summer Schools, 1973.
- [29] Pavlov, D. *Structure-Preserving Discretization of Incompressible Fluids*. Thesis, Caltech, 2009.
- [30] Pavlov D., Mullen P., Tong Y., Kanso E., Marsden J. E., and Desbrun M. [2011], Structure-preserving discretization of incompressible fluids, *Physica D*, **240**(6), 443–458.
- [31] Rockafellar, R. T. [1970] *Convex analysis*, Princeton Univ. Press, Princeton.
- [32] Rockafellar, R. T. [1973] *Penalty methods and augmented Lagrangians in nonlinear programming*, in Fifth Conference on Optimization Techniques, R. Conti and A. Ruberti (eds.), Springer-Verlag, 1973, 518–525.
- [33] Rockafellar, R. T. [1993], Lagrange multipliers and optimality, *SIAM Review* **35**(2), 183–238.
- [34] Rockafellar, R. T. and Wets, R. J.-B. [1998], *Variational Analysis*, Grundlehren der Mathematischen Wissenschaften, **317**, Springer-Verlag, Berlin, 1998.
- [35] Soulaïmani, A., Fortin, M., Dhatt, G., and Ouetlet, Y. [1991], Finite element simulation of two- and three-dimensional free surface flows, *Comput. Meth. in Appl. Mech. Eng.*, **86**, 265–296.